

The impact of
sedimentary
alkalinity release on
the water column
CO₂ system

H. Brenner et al.

The impact of sedimentary alkalinity release on the water column CO₂ system in the North Sea

H. Brenner¹, U. Braeckman², M. Le Guitton¹, and F. J. R. Meysman^{1,3}

¹Department of Ecosystem Studies, Royal Netherlands Institute for Sea Research (NIOZ), Korrिंगaweg 7, 4401 NT Yerseke, the Netherlands

²Marine Biology Research Group, Ghent University, Krijgslaan 281 S8, 9000 Gent, Belgium

³Department of Analytical, Environmental and Geochemistry, Free University of Brussels (VUB), Pleinlaan 2, 1050 Brussels, Belgium

Received: 9 July 2015 – Accepted: 14 July 2015 – Published: 7 August 2015

Correspondence to: H. Brenner (heiko.brenner@nioz.nl)

Published by Copernicus Publications on behalf of the European Geosciences Union.

Title Page

Abstract

Introduction

Conclusions

References

Tables

Figures

◀

▶

◀

▶

Back

Close

Full Screen / Esc

Printer-friendly Version

Interactive Discussion

Abstract

Recently, it has been proposed that alkalinity release from sediments can play an important role in the carbonate dynamics on continental shelves, lowering the $p\text{CO}_2$ of seawater and hence increasing the CO_2 uptake from the atmosphere. To test this hypothesis, sedimentary alkalinity generation was quantified within permeable and muddy sediments across the North Sea during two cruises in September 2011 (basin-wide) and June 2012 (Dutch coastal zone). Benthic fluxes of alkalinity (A_T) and dissolved inorganic carbon (DIC) were determined using shipboard closed sediment incubations. These results show that sediments can be an important source for alkalinity, particularly in the shallow southern North Sea, where high A_T and DIC fluxes were recorded in near shore sediments of the Belgian, Dutch and German coastal zone. In contrast, fluxes of A_T and DIC are substantially lower in the deeper, seasonally stratified, northern part of the North Sea. Overall, our results show that sedimentary alkalinity generation should be considered an important factor in the CO_2 dynamics of shallow coastal systems.

1 Introduction

Coastal seas play a crucial role in the global carbon cycle by connecting the terrestrial, oceanic and atmospheric reservoirs (Regnier et al., 2013). Although continental shelves cover only 7% of the total global ocean surface, they are estimated to account for up to 30% of the oceanic primary production (Gattuso et al., 1998) and between 10 and 25% of the current day oceanic CO_2 uptake (Regnier et al., 2013; Liu et al., 2010). In general, most open shelves in the temperate and high-latitude regions seem undersaturated with respect to atmospheric CO_2 , while the low-latitude shelves generally tend to be supersaturated (Chen and Borges, 2009). However, this rule is far from absolute. Although temperate coastal areas are generally acting as a CO_2 sink, considerable variability has been observed in the CO_2 uptake within and between systems,

The impact of sedimentary alkalinity release on the water column CO_2 system

H. Brenner et al.

Title Page

Abstract

Introduction

Conclusions

References

Tables

Figures

◀

▶

◀

▶

Back

Close

Full Screen / Esc

Printer-friendly Version

Interactive Discussion



The impact of sedimentary alkalinity release on the water column CO₂ system

H. Brenner et al.

[Title Page](#)

[Abstract](#)

[Introduction](#)

[Conclusions](#)

[References](#)

[Tables](#)

[Figures](#)

[◀](#)

[▶](#)

[◀](#)

[▶](#)

[Back](#)

[Close](#)

[Full Screen / Esc](#)

[Printer-friendly Version](#)

[Interactive Discussion](#)

which may be explained by a dominance of different drivers of CO₂ uptake. High nutrient inputs from land fuel intense primary production and hence stimulate atmospheric CO₂ uptake, while respiration of organic matter exported from terrestrial ecosystems stimulates the release of CO₂ in coastal areas (Bozec et al., 2006; Jönsson et al., 2011; Schiettecatte et al., 2007). In addition to these biological sinks and sources, the effect of temperature on the CO₂ solubility controls the magnitude and direction of the CO₂ exchange between coastal waters and the atmosphere (Kitidis et al., 2012; Borges and Frankignoulle, 2003). Therefore the question remains as to what particular drivers are governing the CO₂ dynamics in a given coastal system (Borges and Frankignoulle, 2003).

In addition to water column processes, sediments have also been suggested to play a role, as the shallowness of coastal seas permits a close interaction between the sediment, the water body and the atmosphere. Coastal water bodies are characterized by either a permanently or seasonally mixed water column, which hence establishes a direct link between the sediment and the atmosphere, acting on a time scale of days to months. In contrast, in the open ocean, the sediment and the atmosphere can only interact over much longer time scales (≈ 1000 yr of global oceanic circulation). However, the extent to which sediment geochemistry plays a role in the CO₂ uptake of coastal system remains largely unresolved.

It has been proposed that alkalinity generation caused by anaerobic organic matter degradation in shallow coastal sediments can increase the CO₂ buffer capacity of coastal waters and therefore increase atmospheric CO₂ uptake. When coining this hypothesis, Thomas et al. (2009) estimated that alkalinity generation in Wadden Sea sediments could be responsible for 20–25% of the total CO₂ uptake of the entire North Sea. In the East China Sea it was already suggested by Chen and Wang (1999) that alkalinity generation due to anaerobic degradation processes in sediments adds considerably to the total alkalinity budget in this area. Furthermore, Chen (2002) proposed that shelf-generated alkalinity release from benthic anaerobic processes could be almost as important as alkalinity generated by dissolution of carbonates in the open

The impact of sedimentary alkalinity release on the water column CO₂ system

H. Brenner et al.

Title Page

Abstract

Introduction

Conclusions

References

Tables

Figures

◀

▶

◀

▶

Back

Close

Full Screen / Esc

Printer-friendly Version

Interactive Discussion



ocean. Finally, based on modeled nitrogen and carbon budgets for the northwestern North Atlantic continental shelf, Fennel (2010) suggested that shelf sediments must be an important source of alkalinity. However, Hu and Cai (2011a) obtained a much smaller alkalinity flux from global coastal sediments based on the upscaling of local denitrification and sulfate reduction rates. They concluded that sedimentary alkalinity fluxes are too low to significantly affect the alkalinity budget of the global ocean, but also stated that sedimentary anaerobic processes could be important on regional scales as an alkalinity release mechanism. From these results, it is clear that currently, there is uncertainty as to what extent coastal sediments are an important source of alkalinity to coastal oceans.

In this study, we aim to quantify sedimentary alkalinity generation within various sediment-types in the North Sea. During two cruises samples were collected in September 2011 (basin-wide) and June 2012 (Dutch coastal zone). Benthic fluxes of alkalinity, dissolved inorganic carbon and oxygen were determined using closed sediment incubations and microsensors profiling. Subsequently, we analysed the sources of the observed sedimentary alkalinity release, and after implementing an alkalinity budget for both water column and sediment, we constrained the *net* CO₂ uptake from the atmosphere associated with the sedimentary alkalinity release.

2 Materials and methods

2.1 North Sea system

In this paper we divide the North Sea into three different hydrogeographical zones: the southern North Sea (SNS), the northern North Sea (NNS) and the Skagerrak and the Norwegian Trench (SKNT). The SNS encompasses the Southern Bight (between Belgium/Netherlands and the UK), the shallow Wadden Sea (running along the Dutch and German coast up to Esbjerg in Denmark), the German Bight, and the central part of the North Sea (Fig. 1). The major difference between the SNS and the NNS is the

The impact of sedimentary alkalinity release on the water column CO₂ system

H. Brenner et al.

[Title Page](#)

[Abstract](#)

[Introduction](#)

[Conclusions](#)

[References](#)

[Tables](#)

[Figures](#)

[⏪](#)

[⏩](#)

[◀](#)

[▶](#)

[Back](#)

[Close](#)

[Full Screen / Esc](#)

[Printer-friendly Version](#)

[Interactive Discussion](#)

stratification regime. Whereas the shallow SNS has a fully mixed water column throughout the year, the NNS is thermally stratified in summer, but fully mixed during winter, due to strong wind forcing and surface cooling (Elliott et al., 1991). As the operational border between the SNS and NNS, we use the 100 m depth bathymetric isoline, as employed in previous studies (Pätsch and Kühn, 2008). The third hydrogeographical zone constitutes the Skagerrak and the Norwegian Trench (SKNT), which forms one of the major sediment depositional areas of the North Sea (de Haas and van Weering, 1997). The Skagerrak is part of the transition area that connects the North Sea with the Baltic Sea. It is a rather small strait (200 by 100 km) between the southeast coast of Norway, the southwest coast of Sweden, and the Jutland peninsula of Denmark. The average depth of the Skagerrak is about 210 m. The Skagerrak is strongly stratified in summer, but also features a weak stratification in winter driven by Baltic freshwater inputs (Gustafsson and Stigebrandt, 1996; Rodhe, 1987). The Skagerrak is connected to the Norwegian Sea through the Norwegian trench with a sill depth of 270 m. The Norwegian Trench itself is a deep sedimentary basin (250–700 m) that reaches from the Oslofjord in the southeast to the Stad peninsula in the northwest up (Rodhe, 1996). Like the Skagerrak, the Norwegian Trench is characterized by haline stratified water masses (Reid and Edwards, 2001).

The water transport in the NNS is dominated by the large open boundary with the North Atlantic in the north. Water entering through the Shetland Channel and the Faire Island Channel turns eastwards and leaves the North Sea via the Norwegian Trench in the east. The residence time of the water is about one year. Generally, water entering the NNS does not influence the SNS, as just 5% of the North Atlantic water entering the northern boundary reaches the SNS (Lenhart and Pohlmann, 1997). The water transport in the SNS is mainly determined by inflow of Atlantic Ocean through the English Channel, which mixes with low salinity water coming from rivers and moves along the eastern coastlines towards the north-east. Baltic Sea water entering through the Kattegat and coastal run-off are important in maintaining the Norwegian Coastal Current that initiates in the Skagerrak. This northwards directed current is the only outflow

The impact of sedimentary alkalinity release on the water column CO₂ system

H. Brenner et al.

[Title Page](#)

[Abstract](#)

[Introduction](#)

[Conclusions](#)

[References](#)

[Tables](#)

[Figures](#)

[⏪](#)

[⏩](#)

[◀](#)

[▶](#)

[Back](#)

[Close](#)

[Full Screen / Esc](#)

[Printer-friendly Version](#)

[Interactive Discussion](#)



of the North Sea and thus balances all incoming water inputs as described above. Additionally, the shallow SNS is influenced by a strong tidally induced currents and mixing (Dauwe, 1999). The tides in the SNS are diurnal, whereas maximum surface currents at spring tide occur on the western and southern parts of the SNS. More the the north and into the German Bight, the tidal current velocities decrease (Van der Molen, 2002).

The seafloor of the North Sea predominantly consists of permeable sediments. Medium and fine sand is the main sediment type and occupies the largest part of the North Sea basin. Coarse sand is found at confined locations throughout the entire North Sea basin with larger areas of coarse grained sediments present along the English coast and in front of the German and Danish coasts. Mud and sandy mud are mainly found in the deep trenches along the Norwegian coast, off the coast of Scotland, in particular locations along the Belgian coast and in smaller areas north and east of the German Bight (Lüders, 1955; Schlüter and Jerosch, 2009; Braeckman et al., 2014).

2.2 Sediment sampling

During a cruise onboard RV *Pelagia* in September 2011 we sampled a total of 19 stations across the whole North Sea basin (Table 1). On a second cruise in June 2012, we sampled 7 stations along a transect perpendicular to the Dutch coast from the Wadden island of Terschelling up to the Oyster Grounds in the central North Sea (1b–7b in Fig. 1). Sediment cores were collected at each site using a Reineck box corer. Polymethyl methacrylate (PMMA) core barrels (19 cm inner diameter) were subsequently inserted into the sediment of the box core to a depth of 10 to 15 cm enclosing 15 to 20 cm of overlying water. The cores were excavated from the box core, closed off with a lid at the bottom and immediately transferred into a water-filled reservoir in a thermo-controlled container that was kept at in-situ bottom water temperature. These sediment cores were subsequently used for closed core flux incubations as described below.

During the September 2011 cruise, small sediment cores were retrieved for solid phase analysis and microsensor profiling and these were taken from the same box core as the flux cores. For solid phase analysis, acrylic core barrels (5 cm i.d.) were

The impact of sedimentary alkalinity release on the water column CO₂ system

H. Brenner et al.

Title Page

Abstract

Introduction

Conclusions

References

Tables

Figures

◀

▶

◀

▶

Back

Close

Full Screen / Esc

Printer-friendly Version

Interactive Discussion

inserted into the sediment of the box core. The upper 10 cm of each core was sliced in 1 cm intervals and sediment samples were analyzed for porosity and grain size distribution. Porosity was determined by weight loss after freeze-drying, accounting for salt precipitation in the saline pore water. Grain size distribution was determined using a Malvern Mastersizer 2000 particle analyzer.

For O₂ and pH microsensor profiling, acrylic core liners (3 cm i.d.) were inserted into the sediment of the box core, and afterwards, the sediment was brought level to the rim of the core liner. Cores were subsequently placed in an aquarium containing bottom water at in-situ temperature, which was constantly bubbled with ambient air. Bottom water to top up sediment cores for flux measurements was retrieved by casts with 25 L Niskin bottles (Ocean Test Equipment/Fort Lauderdale, USA) retrieving water at approximately 1 m above the sediment surface. A conductivity, temperature, depth (CTD) was mounted on a standard rosette frame together with 24 Niskin bottles. The CTD was equipped with a SBE3+ thermometer, a SBE4 conductivity meter and a SBE43 dissolved oxygen sensor (Seabird, USA).

2.3 Solute flux measurements

Flux chamber incubations are potentially susceptible to various methodological artifacts resulting from sediment enclosure, which relate to the sensitivity of benthic fluxes to changes in ambient hydrodynamics and altered benthic faunal activity (Santschi et al., 1991; Tengberg et al., 2005; Lehrter et al., 2011). In permeable sediments, fluxes are particularly susceptible to the imposed stirring regime and the associated local pressure gradients that are generated in the flux chamber, which drive the advective pore water exchange between sediment and overlying water (Huettel and Gust, 1992; Janssen et al., 2005). The flux chamber type employed here was based on the design as in Huettel and Gust (1992), which was specifically developed for flux studies in permeable sediments. The sediment cores retrieved were closed off with a PMMA top lid that was equipped with a large central stirring disc (diameter: 14 cm). The rotation of the disc mixes the overlying water and establishes a specific radial pressure

The impact of sedimentary alkalinity release on the water column CO₂ system

H. Brenner et al.

Title Page

Abstract

Introduction

Conclusions

References

Tables

Figures

◀

▶

◀

▶

Back

Close

Full Screen / Esc

Printer-friendly Version

Interactive Discussion



gradient, which drives pore water exchange in the chamber. A major challenge for flux chamber studies in permeable sediments is the selection of the appropriate stirring regime. Without knowledge of the local in-situ hydrodynamics, it is impossible to predict a priori which stirring regime is appropriate for a given site. Here we used two different stirring rates at each station (40 and 80 RPM), to mimic a range of interfacial pressure gradients and solute exchange conditions (Huettel and Gust, 1992; Janssen et al., 2005; Rao et al., 2012). By taking this approach, we are able to discern how sensitive the fluxes at each station are to advective exchange, and thus, we get an idea of the uncertainty on our flux estimates for the permeable sites that we visited.

Prior to the start of the flux measurements, the overlying water in each core was replaced with ambient bottom water to ensure that the chemical composition of the overlying water closely resembled in-situ conditions. Each set of flux measurements began by securing gas-tight lids equipped with O-ring seals on each core. Core lids contained two sampling ports on opposite sides for subsampling during the incubation and these ports were carefully purged with bottom water prior to the start of each incubation to remove any air bubbles trapped. Fiber-optical oxygen sensors (FireSting OXF1100) were inserted into a third opening in the top lid. The chambers were closely inspected to ensure that no gas bubbles remained inside the chamber. Two or three replicate chamber incubations were made per station.

The temporal evolution of the oxygen concentration in the overlying water of the flux chambers was continuously monitored using oxygen optodes at a sample interval of 1 min. Optodes were pre-calibrated on the same day using a two-point calibration with ambient seawater at 0% (saturated with sodium sulphite) and 100% O₂ saturation (bubbled with air). Optode results were verified with measurements of the O₂ concentration by Winkler titration in discrete water samples before and after incubation (Grasshoff et al., 2009).

A water subsample (~ 50 mL) was withdrawn from the chambers at 4–6 h intervals for solute analysis as described below. When a water sample was extracted via one sampling port, an equal amount of ambient bottom water entered through the replace-

The impact of sedimentary alkalinity release on the water column CO₂ system

H. Brenner et al.

Title Page

Abstract

Introduction

Conclusions

References

Tables

Figures

◀

▶

◀

▶

Back

Close

Full Screen / Esc

Printer-friendly Version

Interactive Discussion



ment tube connected to the other sampling port. Samples were collected in plastic syringes for alkalinity (A_T) and in glass syringes for dissolved inorganic carbon (DIC) analysis. Water samples for A_T (~ 10 mL) were filtered ($0.45 \mu\text{m}$ Millex-HA syringe filter) and stored in the dark at 4°C . DIC water samples (~ 12 mL) were not filtered, but
5 poisoned with $10 \mu\text{L}$ HgCl_2 and stored submerged at 4°C in a fridge.

The Total Oxygen Uptake (TOU) rate and the flux of DIC and A_T were determined from a linear regression of overlying water concentrations vs. incubation time (Eq. 1).

$$J = \frac{V_{\text{ow}}}{A} \frac{dC_{\text{ow}}}{dt} \quad (1)$$

At the end of the incubation, the top lid was removed, and the height of the overlying
10 water ($H = V_{\text{ow}}/A$) was measured at four points along the side of the core using a ruler and the mean height was calculated. Glud (2008) suggested that an oxygen decrease by more than 10–15% from the initial conditions can already stimulate processes that cause a non-linear decrease in oxygen concentrations, which also might affect other solute fluxes across the sediment–water interface. Here we found that the linear regressions used to calculate the oxygen uptake were insensitive to an oxygen decrease
15 of 30% or more (for examples see Fig. 3).

2.4 Analytical methods

Total A_T was determined via an open-cell titration procedure, using a Metrohm Titrando 888 system with a combined Metrohm glass electrode (Unitrode) following the procedure SOP3a as described in Dickson et al. (2007). Samples (10 mL) were placed in a temperature regulated open cell (25°C) and titrated with a solution of hydrochloric acid (0.1 N) in a two-stage process. First the sample (10 mL) was acidified to a pH close to 3.5 and then titrated in small steps down to a pH of 3.0. Subsequently, A_T was calculated using a non-linear regression approach based on SOP3a from Dickson et al. (2007). Two replicate measurements were carried out for each sample analyzed.
25 Titrations ($n = 10$) of Certified Reference Materials (CRM Batch 116 provided by A. G.

Dickson) were on average within $4 \mu\text{mol kg}^{-1}$ of the nominal value with a precision of $5 \mu\text{mol kg}^{-1}$.

DIC was determined using an AS-C3 DIC analyzer (Apollo SciTEch, USA), in which the sample (10 mL) was acidified and the released CO_2 was detected using a solid state infra-red CO_2 detector (LI-7000, LI-COR Biosciences, USA). Two replicate measurements were carried out for each sample analyzed. Quality assurance of the DIC analysis was also based on CRM (Batch 116 – accuracy and precision: $3 \mu\text{mol kg}^{-1}$).

2.5 O_2 and pH microprofiling

Microsensor profiling was performed using commercial Clark-type O_2 and potentiometric pH microsensors operated with a motorized micromanipulator (Unisense A.S., Denmark). Vertical depth profiles of O_2 were recorded using an electrode with a tip size of $100 \mu\text{m}$ at $250 \mu\text{m}$ steps, beginning at 2 mm above the sediment–water interface until either anoxia or 20 mm depth. The O_2 microsensors were calibrated with a 2-point calibration made in air-saturated seawater (100 % saturation) and at depth in anoxic sediment (0 % saturation). Depth profiles of pH were measured using microsensors with a tip size of $200 \mu\text{m}$ in 1 mm steps, beginning 4 mm above the sediment surface until 35 mm depth. Measurements were always started within 1 h after sampling. The pH microsensors were calibrated using NBS buffers (pH 4 and 7) and TRIS buffer (Delvalls and Dickson, 1998), and the pH is reported on the total scale.

The diffusive oxygen uptake (DOU) of the sediment was calculated from the O_2 depth profiles as

$$\text{DOU} = -D_{\text{O}_2} \frac{d[\text{O}_2]}{dz} \quad (2)$$

where z is the depth and $[\text{O}_2]$ denotes O_2 concentration. Profiles were measured under diffusive conditions and the slope $d[\text{O}_2]/dz$ was determined from the gradient in the diffusive boundary layer (Glud, 2008). The molecular diffusion coefficient of O_2 in

BGD

12, 12395–12453, 2015

The impact of sedimentary alkalinity release on the water column CO_2 system

H. Brenner et al.

Title Page

Abstract

Introduction

Conclusions

References

Tables

Figures

◀

▶

◀

▶

Back

Close

Full Screen / Esc

Printer-friendly Version

Interactive Discussion



seawater (D_{O_2}) was calculated as a function of the bottom water salinity and temperature using the *CRAN:marelac* extension package in the open-source programming language R (Soetaert et al., 2010).

2.6 Statistical analyses

5 Results are reported as the mean ± 1 standard deviation (SD) of n replicate measurements. Nonparametric statistics were used in the interpretation of results, including the Mann–Whitney U test (p) for comparison of the mean of two independent groups of measurements, and the Spearman’s rank correlation coefficient (ρ) as a measure of the statistical dependence between two variables. Statistical analyses were conducted
10 in R using the *CRAN:stats* package.

3 Results

3.1 Bottom water characteristics

Bottom water salinity, temperature and oxygen concentration as obtained by CTD profiling are listed in Table 1, and characteristic temperature depth profiles are displayed
15 in Fig. 2. Bottom water salinity and temperature of stations from the basin wide North Sea cruise ranged from 35.39 PSU (NNS) to 29.35 PSU (SNS) and 17.41 °C (SNS) to 6.02 °C (NNS). The bottom water in the NNS and SKNT was generally colder and more saline than bottom water in the SNS (Mann–Whitney; Temperature: $p = 0.001$; Salinity: $p < 0.001$). A thermocline was formed between between 20–50 m water depth in all
20 stations of the NNS and SKNT, but just in two stations of the SNS (Fig. 2 and Table 1). The bottom water oxygen concentrations did however not exhibit significant differences between the SNS and other parts of the North Sea (Mann–Whitney; $p > 0.5$).

The impact of sedimentary alkalinity release on the water column CO₂ system

H. Brenner et al.

Title Page

Abstract

Introduction

Conclusions

References

Tables

Figures

◀

▶

◀

▶

Back

Close

Full Screen / Esc

Printer-friendly Version

Interactive Discussion

3.2 Sediment properties

The median grain size for all stations visited during the basin wide North Sea campaign in 2011 ranged from 21 to 499 μm (mean median grain size: 215 μm). In the SNS the median grain size ranged from 138–499 μm (mean median grain size: 215 μm), and according to the Wentworth scale, the SNS sediments can be classified as fine to medium sand (Table 1). Sediments in the NNS (median grain size range 119–314 μm ; mean 227 μm) were not significantly different from the SNS (Mann–Whitney; $p = 0.8$), hence also classifying as fine to medium sand. In contrast, sediments from the Skagerrak and Norwegian Trench (SKNT) were considerably finer (Mann–Whitney; $p < 0.01$), with the median grain size ranging from 22–62 μm . Thus, sediments of SKNT classified as fine to coarse silt on the Wentworth scale (Table 1).

Porosity for all stations in the North Sea basin varied from 0.32 to 0.74. Between sediments of the SNS (mean: 0.34) and NNS (mean: 0.37) no significant differences in porosity were found (Mann–Whitney; $p = 0.31$). However, sediments of the SKNT displayed a significantly higher porosity than sediments from the SNS or NNS (Mann–Whitney; $p < 0.05$).

3.3 Benthic flux chamber incubations

The temporal evolution of the solute concentrations (O_2 , DIC and A_T) in the overlying water from flux chamber incubations at representative stations from each of the three zones (SNS, NNS, SKNT) is presented in Fig. 3. The oxygen data display a linear decrease, while the DIC and A_T data display an increasing trend, albeit with greater variability due to the limited number of subsamples. Fluxes were only considered if their calculation is based on a linear regression of at least 4 points combined with an r^2 value greater than 0.8. Furthermore, fluxes were set to zero in case the slope of the linear regression was not significantly different from zero.

During the basin-wide campaign in September 2011, TOU rates ranged from 3.1 to 28.7 $\text{mmol m}^{-2} \text{d}^{-1}$ for the SNS, 0.7 to 6.2 $\text{mmol m}^{-2} \text{d}^{-1}$ for the NNS and 2.9 to

BGD

12, 12395–12453, 2015

The impact of sedimentary alkalinity release on the water column CO_2 system

H. Brenner et al.

Title Page

Abstract

Introduction

Conclusions

References

Tables

Figures

◀

▶

◀

▶

Back

Close

Full Screen / Esc

Printer-friendly Version

Interactive Discussion



The impact of sedimentary alkalinity release on the water column CO₂ system

H. Brenner et al.

[Title Page](#)

[Abstract](#)

[Introduction](#)

[Conclusions](#)

[References](#)

[Tables](#)

[Figures](#)

[⏪](#)

[⏩](#)

[◀](#)

[▶](#)

[Back](#)

[Close](#)

[Full Screen / Esc](#)

[Printer-friendly Version](#)

[Interactive Discussion](#)

5.7 mmol m⁻² d⁻¹ for the SKNT. During the Dutch transect cruise in June 2012, TOU rates ranged from 6.5 to 25.1 mmol m⁻² d⁻¹ (Table 2). Thereby, the highest oxygen up-take rates were measured in the SNS, followed by the SKNT, while the lowest TOU rates were measured in the NNS (mean value SNS: 10.0 mmol m⁻² d⁻¹ in 2011 and 13.5 mmol m⁻² d⁻¹ in 2012; SKNT: 3.9 mmol m⁻² d⁻¹; NNS: 3.4 mmol m⁻² d⁻¹). In general, TOU rates in the SNS are significantly higher than TOU rates of the NNS and the SKNT (Mann–Whitney; *NNS*: $p < 10^{-5}$; SKNT: $p < 0.001$). Between TOU rates from the NNS and TOU rates from the SKNT no statistical difference could be identified (Mann–Whitney; $p = 0.6$). Furthermore, TOU rates measured in the SNS in June 2012 are not significantly different from TOU rates measured in September 2011 (Mann–Whitney; $p > 0.05$).

Within the permeable sediments of the SNS and NNS, flux chamber incubations were performed at two different stirring speeds (40 and 80 RPM). In general, the TOU rates were about 80 % higher at the higher stirring speed (Fig. 4a), indicating an advective dominated transport within the sediments (Spearman's; $p < 0.01$). On the other hand, a correlation between median grain size of the sediments and TOU rates could not be confirmed (Fig. 4b).

In general, A_T and DIC concentrations increased linearly with time in the overlying water of the flux incubations for most stations. A_T fluxes for both campaigns ranged from 0 to 21.4, 0 to 3.0 and 1.4 to 9.9 mmol m⁻² d⁻¹ for the SNS, NNS and SKNT respectively. The highest A_T fluxes were observed in the SNS (mean: 6.5 mmol m⁻² d⁻¹ in 2011 and 5.7 mmol m⁻² d⁻¹ in 2012) and in the SKNT (4.3 mmol m⁻² d⁻¹). The lowest mean A_T flux was calculated for the NNS (1.8 mmol m⁻² d⁻¹). Only the A_T fluxes of the SNS are significantly higher than A_T fluxes of the NNS (Mann–Whitney; SNS: $p < 0.001$; SKNT: $p = 0.2$). A_T fluxes measured during the basin wide cruise in 2011 are similar to those measured along the Dutch transect in 2012 (Mann–Whitney; $p = 0.3$).

DIC fluxes varied between 1.5–29.1, 0–6.2 and 4.2–7.2 mmol m⁻² d⁻¹ for the SNS, NNS and SKNT respectively. The trends in DIC flux were similar as those obtained for the TOU rates and A_T fluxes. The highest DIC fluxes were measured in the SNS,

followed by the SKNT and the NNS (mean: SNS: $11.5 \text{ mmol m}^{-2} \text{ d}^{-1}$ in 2011 and $12.3 \text{ mmol m}^{-2} \text{ d}^{-1}$ in 2012; SKNT: $6.1 \text{ mmol m}^{-2} \text{ d}^{-1}$; NNS: $0.9 \text{ mmol m}^{-2} \text{ d}^{-1}$). DIC fluxes were significantly higher in the SNS than in the NNS, but showed no differences to the DIC fluxes measured in the SKNT (Mann–Whitney; NNS: $p < 0.01$; SKNT: $p = 0.3$), while also no significant difference was found between DIC fluxes of the SKNT and the NNS (Mann–Whitney; $p = 0.08$). As found for TOU rates and A_T fluxes, the DIC fluxes in the SNS were similar between both campaigns (Mann–Whitney; $p = 0.7$). This allows us to examine all solute fluxes recorded in the SNS as one single group in the discussion section.

3.4 O₂ and pH microprofiling

Representative examples of O₂ and pH depth profiles in stations from all three zones of the North Sea are presented in Fig. 5. In some stations pore water profiles could not be measured due to the coarse grain size and the presence of carbonate shell fragments, which induces a high risk of damaging the microsensors. In general, pore water O₂ declines as a result of O₂ consumption associated with organic matter degradation. From the O₂ depth profiles the DOU rates of the sediments were calculated as detailed in Sect. 2.5. In the SNS, DOU rates ranged from 0.20 to $6.95 \text{ mmol m}^{-2} \text{ d}^{-1}$, while in the NNS and SKNT, a range of 1.47 to $4.33 \text{ mmol m}^{-2} \text{ d}^{-1}$ and 0.83 to $2.49 \text{ mmol m}^{-2} \text{ d}^{-1}$ were found (Table 3). The lowest mean DOU rate was measured in the SKNT, followed by the DOU rates of the NNS and SNS (SKNT: $1.77 \text{ mmol m}^{-2} \text{ d}^{-1}$, NNS: $2.20 \text{ mmol m}^{-2} \text{ d}^{-1}$; SNS: $2.39 \text{ mmol m}^{-2} \text{ d}^{-1}$).

The oxygen penetration depth (OPD) is defined as the thickness of the oxic zone in marine sediments (Cai and Sayles, 1996), and was operationally defined as the depth below which the O₂ concentration drops below $1 \mu\text{mol kg}^{-1}$. In some permeable sediments, the oxygen did not fully deplete over the measured depth profiles (first 2 cm), and so the OPD could not be determined. In the remaining cores, the OPD

BGD

12, 12395–12453, 2015

The impact of sedimentary alkalinity release on the water column CO₂ system

H. Brenner et al.

Title Page

Abstract

Introduction

Conclusions

References

Tables

Figures

◀

▶

◀

▶

Back

Close

Full Screen / Esc

Printer-friendly Version

Interactive Discussion

was as shallow as 5.3 mm for the SNS, 3.20 mm for the SKNT and 7.10 mm for the NNS.

Table 3 compares the TOU with the corresponding DOU for the basin-wide campaign in September 2011. The TOU/DOU ratio ranged from 50.1 (SNS) to 1.1 (NNS), and DOU rates were significantly lower than TOU rates (Spearman's; $p < 0.01$), indicating that physical or biological driven advective transport strongly enhanced the sedimentary oxygen uptake.

Depth pH profiles of representative cores are presented in Fig. 5. Depth profiles generally show a decline of pH in all profiled cores, which can be attributed to the release of CO_2 resulting from organic matter degradation. Furthermore, the cores from the NNS and SKNT were typically characterized by a sub-surface minimum in pH, while the depths of these pH minima matched the corresponding OPD. Hence, we interpret these sub-surface pH minima as resulting from the aerobic oxidation of reduced substances transported upwards from deeper sediment layers. Generally, the pH increased again at depth in the cores, most likely due to A_T generation associated with the anoxic degradation of organic matter (see discussion below).

4 Discussion

4.1 Benthic mineralization in the North Sea

Several studies have previously addressed benthic oxygen consumption in the North Sea, although most studies are restricted to the southern North Sea (Table 4). The TOU rates found in the present study for the North Sea (range 3.1–28.7 $\text{mmol O}_2 \text{m}^{-2} \text{d}^{-1}$) fall within the range of previously published TOU rates (range 0–57.1 $\text{mmol O}_2 \text{m}^{-2} \text{d}^{-1}$), which is however large. Due to temporal variability (seasonality), spatial variability (e.g. substrates ranging from cohesive mud to highly permeable sand), but also differences in methodology (see discussion below on the impact of stirring rate), it remains difficult to intercompare the oxygen consumption rates that have been obtained in different

The impact of sedimentary alkalinity release on the water column CO_2 system

H. Brenner et al.

Title Page

Abstract

Introduction

Conclusions

References

Tables

Figures

◀

▶

◀

▶

Back

Close

Full Screen / Esc

Printer-friendly Version

Interactive Discussion

studies. So despite this growing database of TOU rates, a more accurate assessment of the spatial and temporal variation of the oxygen consumption in the North Sea remains an outstanding challenge.

In our basin wide campaign in 2011, we obtained the highest mean TOU rate in the SNS ($10.0 \text{ mmol m}^{-2} \text{ d}^{-1}$), followed by the SKNT ($3.9 \text{ mmol m}^{-2} \text{ d}^{-1}$), while the lowest TOU rates were measured in the NNS ($3.4 \text{ mmol m}^{-2} \text{ d}^{-1}$). One important environmental factor in controlling the TOU rates is the amount of primary production in these different regions. Part of this organic matter produced during photosynthesis is respired in the water column, while the remaining part sinks down to the sediments and undergoes respiration there. As oxygen serves as the ultimate electron acceptor for almost all respired organic carbon (Thamdrup and Canfield, 2000), high primary production rates tend to relate to high TOU rates in the sediments. Note, that besides primary production rates, also the water depth and thereby the amount of organic carbon which reaches the sediments is of great importance. Because of the shallow water depth, the fraction of organic carbon which reaches the sediments in the southern North Sea is considerably higher than in the northern North Sea, hence further increasing the TOU rates in this region (Kühn et al., 2010). Based on measured surface chlorophyll concentration in the southern North Sea, Joint and Pomroy (1993) estimated primary production rates for a period from August 1988 to October 1989, and found clear regional differences in primary production in the SNS ranging from $18 \text{ mmol C m}^{-2} \text{ d}^{-1}$ along the British Coast to $59 \text{ mmol m}^{-2} \text{ d}^{-1}$ in the German Bight. A model study by Moll (1998) covering the whole North Sea confirmed the large regional variation in depth-integrated annual primary production rates ranging from $21 \text{ mmol C m}^{-2} \text{ d}^{-1}$ in the NNS to $79 \text{ mmol C m}^{-2} \text{ d}^{-1}$ in the German Bight of the SNS. TOU rates observed are congruent with these previous observational and modelling studies, with high values in the southern North Sea, and in particular in the German Bight, to lower values in the northern North Sea.

A second important environmental factor controlling the north–south gradient in TOU rates could be summer bottom water temperature. In a recent seasonal flux study of

BGD

12, 12395–12453, 2015

**The impact of
sedimentary
alkalinity release on
the water column
CO₂ system**

H. Brenner et al.

Title Page

Abstract

Introduction

Conclusions

References

Tables

Figures

◀

▶

◀

▶

Back

Close

Full Screen / Esc

Printer-friendly Version

Interactive Discussion

The impact of sedimentary alkalinity release on the water column CO₂ system

H. Brenner et al.

[Title Page](#)

[Abstract](#)

[Introduction](#)

[Conclusions](#)

[References](#)

[Tables](#)

[Figures](#)

[◀](#)

[▶](#)

[◀](#)

[▶](#)

[Back](#)

[Close](#)

[Full Screen / Esc](#)

[Printer-friendly Version](#)

[Interactive Discussion](#)

shallow coastal sediments from the North Sea, a positive correlation was found between benthic solute fluxes and water temperature (Rao et al., 2014). These authors proposed that higher bottom water temperatures in summer are a main driver for higher benthic fluxes as increased temperatures enhance the metabolic activity in the sediment. In September 2011, the thermocline was formed between 20 and 50 m (Fig. 2 and Sect. 3.1), and the whole NNS and SKNT were stratified, while in contrast, the SNS was fully mixed (apart from the stations 38 and 45 on the border with the NNS). As a result, the bottom water in the NNS and SKNT was substantially colder ($\approx 11^\circ\text{C}$ difference between SNS and NNS/SKNT – Table 1). Adopting a temperature Q10 coefficient of ≈ 2 for benthic respiration (Denman and Pena, 2002; Schrum et al., 2006), one hence would expect a doubling of the TOU between the NNS and SNS due to bottom water temperature, all other environmental factors being the same. Accordingly, lower bottom water temperatures in the NNS and SKNT could indeed partially explain the lower TOU values recorded compared to the SNS.

To further identify the drivers of the observed spatial variability across the North Sea, we examined the correlation of TOU rates with water depth, porosity and grain size (Fig. 6). We found significant correlations between TOU values and water depth (Spearman's; $p < 0.01$), suggesting that increased water depth reduced the benthic pelagic coupling in the NNS and SKNT. As more organic matter is remineralized upon the longer transit through the water column, less detritus reaches the seafloor, and this hence decreases the contribution of benthic mineralization in the overall respiration. Finally, we also found both a negative correlation between TOU and porosity (Spearman's; $p < 0.02$) and a significant negative correlation between TOU and median grain size (Spearman's; $p < 0.01$). This opposes the classical picture of sedimentary diagenesis, where high oxygen consumption rates and intense biogeochemical cycling are typically linked to fine-grained organic rich sediments. Instead, we found the highest TOU values in the permeable sediments of mostly the SNS (low porosity, high median grain size), which supports the more recent ideas of permeable sediments as active bio-catalytic filters (Huettel and Rusch, 2000), which actively trap suspended detritus

by means of advective currents through the upper sediment layers and rapidly mineralize this trapped organic matter. As a result, these permeable sediments display low standing stocks of organic matter, but high TOU values.

The importance of advective transport for the benthic oxygen dynamics is emphasized by the deep oxygenation of the surface sediment at permeable sites (Fig. 5a), the impact of benthic chamber stirring speed on the TOU (Fig. 4), and by the strong difference between TOU values as measured by benthic incubations and the corresponding DOU values as obtained by microprofiling (Table 3). We found that DOU values were always smaller than TOU values for all stations throughout the North Sea. In general, the total oxygen uptake can be decomposed as $TOU = DOU + BMU + AMU$ (Glud, 2008), where BMU represents benthos mediated O_2 uptake resulting from burrow irrigation and the respiration of infauna, and AMU represents the enhancement of the sedimentary O_2 uptake by purely physical transport processes, such as pore water advection induced by currents over bottom topography (Huettel and Rusch, 2000; Meysman et al., 2007) and oscillatory pore water mixing induced by waves (Shum, 1992).

A second signature of physical and or biological pore water irrigation is the deep oxygenation of the surface sediment. As already noted above, in some highly permeable sites, the surface sediment remained completely oxygenated over the whole surface layer that was examined by O_2 microsensor profiling (first 20 mm), and so no oxygen penetration depth (OPD) could be determined. For those stations that did allow to determine the OPD (i.e., the pore water O_2 signal decreased to zero), we employed the analytical model of Cai and Sayles (1996), which provides an inverse relation between OPD and DOU (Fig. 7a) (Eq. 3).

$$L = 2\phi D_s \frac{[O_2]_{bw}}{F_{O_2}^0}, \quad (3)$$

In this expression, L is the OPD of the sediment, ϕ is the porosity, and D_s is the effective diffusivity of O_2 in the pore water (i.e., corrected for tortuosity), and $[O_2]_{bw}$. The above relation was used to estimate the theoretical OPD from the measured DOU as shown in

BGD

12, 12395–12453, 2015

**The impact of
sedimentary
alkalinity release on
the water column
 CO_2 system**

H. Brenner et al.

Title Page

Abstract

Introduction

Conclusions

References

Tables

Figures

◀

▶

◀

▶

Back

Close

Full Screen / Esc

Printer-friendly Version

Interactive Discussion



Fig. 7b. The actually measured OPD is systematically larger than the predicted OPD for all stations. As the model 3 holds for sediments that only experience diffusive transport, the discrepancy suggests that non-diffusive transport (i.e. bio-irrigation or physical advection) increases the oxygen availability and penetration in the sediment (Archer and Devol, 1992).

4.2 Benthic DIC release in the North Sea

The benthic DIC release in the North Sea follows the same spatial pattern as the benthic oxygen uptake: the highest DIC effluxes were recorded in the SNS ($11.5 \text{ mmol m}^{-2} \text{ d}^{-1}$ in 2011 and $12.3 \text{ mmol m}^{-2} \text{ d}^{-1}$ in 2012), followed by the SKNT ($6.1 \text{ mmol m}^{-2} \text{ d}^{-1}$) and the NNS ($0.9 \text{ mmol m}^{-2} \text{ d}^{-1}$). However, while TOU values were comparable in NNS and SKNT, the DIC flux in the SKNT was significantly higher than in the NNS. As for the TOU, we found a significant positive correlation between the DIC efflux and water depth (Spearman's; $p = 0.02$), and a weak negative correlation between the DIC efflux and the porosity (Spearman's; $p = 0.07$) and a significant negative correlation between the DIC efflux and median grain size (Spearman's; $p < 0.01$; Fig. 6). Overall, this suggests that the same environmental factors (pelagic primary production, temperature, water depth, sediment permeability) that are driving the TOU are also controlling the spatial pattern of the sedimentary DIC release in the North Sea.

Overall, we found the DIC to be strongly positively correlated with the TOU (Fig. 8; Spearman's; $p < 0.0001$). The ratio between the DIC efflux and the TOU at a given site represents the respiratory quotient (RQ), and we found that the mean RQ value for the SNS (0.95), NNS (0.94) and SKNT (1.00) to be all similar. No significant differences were detected between the three zones (Mann–Whitney; $p > 0.05$). In general, the RQ can be used as an indicator for the degree of reoxidation of reduced compounds associated with anaerobic remineralization (Therkildsen and Lomstein, 1993). Assuming that (1) no carbonate dissolution occurs in the sediment, (2) that the stoichiometry of organic matter follows the Redfield ratio ($C : N : P = 106 : 16 : 1$; Redfield, 1958), and (3) that organic matter is oxidized using oxygen as the sole electron acceptor, one

The impact of sedimentary alkalinity release on the water column CO_2 system

H. Brenner et al.

Title Page

Abstract

Introduction

Conclusions

References

Tables

Figures

◀

▶

◀

▶

Back

Close

Full Screen / Esc

Printer-friendly Version

Interactive Discussion



would obtain an RQ of 0.77 (solid line in Fig. 8; Paulmier et al., 2009). The slope of the regression in the DIC efflux vs. TOU plot equals 0.71 (Fig. 8a), which is close to Redfield ratio.

In principle, the RQ value is expected to increase with increasing importance of suboxic and anoxic respiration pathways, and subsequent accumulation of reduced compounds such as pyrite, as respiration along these pathways is releasing DIC without consuming oxygen. Alternatively, dissolution of carbonates may also lead to an increased RQ due to the release of two moles DIC per mole CaCO_3 dissolved. Equally, the RQ value is expected to decrease when a stock of reduced compounds is being oxidized, i.e., the annihilation of a previously accumulated *oxygen debt*.

4.3 Benthic alkalinity release in the North Sea

Our results show that North Sea sediments can be a substantial source of A_T with sediment effluxes ranging from 0 to $28.7 \text{ mmol Eq m}^{-2} \text{ d}^{-1}$ (Fig. 2). The A_T fluxes reported here were obtained by monitoring the temporal evolution of A_T in the overlying water of enclosed sediment incubations. In the same sediment incubations, Burt et al. (2014) measured the efflux of the short-lived Radium isotopes (^{224}Ra and ^{223}Ra) and subsequently estimated A_T fluxes. To this end, these authors used the Ra-isotope data to estimate the overall water exchange rate between the pore water and the overlying water column. This water exchange rate was then multiplied by the excess concentration of A_T in pore water, which was estimated from pore water analysis. This indirect estimate procedure resulted in benthic A_T fluxes between 4.7 and $22.1 \text{ mmol Eq m}^{-2} \text{ d}^{-1}$, and is in very good agreement with the A_T flux values obtained here (Fig. 9). The disagreement between observed and calculated A_T flux may result from applying the same A_T pore-water concentration for all stations in calculating the A_T fluxes based on Radium-isotope data. This assumption might be wrong and could lead to an over-estimation of the A_T flux in station 38. For a more detailed discussion on the correlation between both methods see Burt et al. (2014).

**The impact of
sedimentary
alkalinity release on
the water column
CO₂ system**

H. Brenner et al.

Title Page

Abstract

Introduction

Conclusions

References

Tables

Figures

◀

▶

◀

▶

Back

Close

Full Screen / Esc

Printer-friendly Version

Interactive Discussion

Gustafsson et al. (2014) estimated that sediments of the Baltic Sea generate A_T with a mean rate of $2.4 \text{ mmol Eq m}^{-2} \text{ d}^{-1}$, which is in the same order as the A_T input by rivers in that basin. As main sources for A_T these authors propose denitrification together with sulfate reduction and/or silicate weathering. Chen and Wang (1999) estimated that sediments in the East China sea generate between 2.9 and $4.9 \text{ mmol Eq m}^{-2} \text{ d}^{-1}$ A_T . Over 80 % of this A_T flux was thereby attributed to iron and sulfate reduction, with no contribution from carbonate dissolution.

Krumins et al. (2013) used a one-dimensional reactive transport model to estimate A_T fluxes from coastal sediments. For that study, the authors divided the global shelf into four different environments, each with distinctive particular organic and inorganic carbon fluxes. Ultimately, they identified non-carbonate shelves (e.g. the North Sea) as an A_T source of $2.7 \text{ mmol Eq m}^{-2} \text{ d}^{-1}$.

On a global scale, Krumins et al. (2013) estimated an A_T flux for the coastal ocean of 29 Tmol yr^{-1} . Whereas this estimate agrees well with an independent estimation by Chen (2002) ($16\text{--}31 \text{ Tmol yr}^{-1}$), Hu and Cai (2011a) obtained a much smaller flux of $4\text{--}6 \text{ Tmol yr}^{-1}$. Note, that all these three studies are based on different assumption on the underlying processes that are generating A_T . Whereas the A_T flux estimated by Chen (2002) is mainly generated by sulfate reduction with zero contribution of carbonate dissolution, Krumins et al. (2013) acknowledged carbonate dissolution as a benthic A_T source. Hu and Cai (2011a) is based on anaerobic A_T generation alone, hence possible contributions by carbonate dissolution are not taken into account. Furthermore, these latter authors treat the coastal sediment–water column system as a single system, while the other two papers only consider the sediment.

To put these different assumptions into perspective, and verify their consequences, we now develop an alkalinity budget for the SNS, in which we first provide a sediment budget, and subsequently, we extend this argument to arrive at a combined sediment and water column alkalinity budget. We restrict this discussion to the SNS, as we have shown in Sect. 3.3 that A_T fluxes in the SNS significantly exceed those of the other two zones. High primary production, riverine input of terrestrial organic matter, and

the shallow water depth favor a high respiration rate in the SNS. Furthermore, in the context of atmospheric CO₂ uptake, a direct link between alkalinity release from the sediments and the atmosphere is needed, which requires a non-stratified water column as encountered in most parts of the SNS.

5 4.4 Sources of alkalinity in sediments of the SNS

The high benthic A_T effluxes observed in the SNS invoke the question as to which processes are generating A_T in the sediment. In the following we will discuss how different biogeochemical pathways contribute to the overall A_T release from sediments, and in this way, we will try to assemble a closed A_T budget for the SNS sea floor. To this end, we developed a simplified biogeochemical model of the SNS sediment, which accounts for carbonate dissolution (CD), aerobic respiration (AR), nitrification (NI), denitrification (DN), iron reduction (IR), sulfate reduction (SR), free sulfide oxidation (SO), and pyrite formation (PF) as biogeochemical pathways. The input parameters, diagenetic relations, and output variables are summarized in Table 5. The A_T/DIC flux ratio for each of these reactions is indicated as a straight line in Fig. 10. In the next paragraphs, we now discuss how the rates of the individual reactions can be constrained based on our flux measurements and literature data.

In theory, the dissolution of one mole of CaCO₃ releases two moles of A_T, assuming no other processes are acting.



The undersaturation of the pore water with respect to the phases of calcium carbonate present (e.g. high Mg calcite, aragonite or calcite) determines the rate at which carbonate will dissolve. In general the undersaturation of the pore water can have two causes (Boudreau et al., 2010): (1) undersaturation of the overlying water and (2) additional undersaturation of the pore water due to metabolic respiration. In the North Sea, the overlying water is always oversaturated with respect to all common carbonate phases (Frankignoulle et al., 1998), and so, dissolution of CaCO₃ in the sediment must

The impact of sedimentary alkalinity release on the water column CO₂ system

H. Brenner et al.

Title Page

Abstract

Introduction

Conclusions

References

Tables

Figures

◀

▶

◀

▶

Back

Close

Full Screen / Esc

Printer-friendly Version

Interactive Discussion



The impact of sedimentary alkalinity release on the water column CO₂ system

H. Brenner et al.

Title Page

Abstract

Introduction

Conclusions

References

Tables

Figures

◀

▶

◀

▶

Back

Close

Full Screen / Esc

Printer-friendly Version

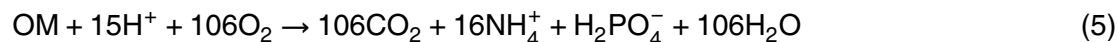
Interactive Discussion



be exclusively metabolically driven. Both the CO₂ production during organic matter mineralization as well as the oxidation of reduced compounds produced during anaerobic respiration processes can make the pore water undersaturated with respect to carbonates, and therefore, fuel metabolic driven dissolution (Jahnke et al., 1994). The increase of the A_7 fluxes with increasing TOU rates (Fig. 8) forms indeed an indication for metabolic driven dissolution of CaCO₃ (Jahnke and Jahnke, 2004).

From the flux dataset available here, it is not possible to constrain the actual CaCO₃ dissolution rate in each station. However, it is still possible to provide an upper limit for the CaCO₃ dissolution rate on a larger geographic scale. Gazeau et al. (personal communication) recently estimated carbonate production in the southern North Sea to be 2.7 mmol C m⁻² d⁻¹. Net carbon burial does not occur in the North Sea, except for small amounts in the Skagerrak and the Norwegian Channel (de Haas et al., 2002; Thomas et al., 2005; Bozec et al., 2006). Therefore, we consider carbonate production and dissolution to be in steady state. Accordingly, carbonate dissolution in sediments can release up to 5.4 mmol Eq m⁻² d⁻¹ of A_7 .

In addition to carbonate dissolution, A_7 generation can be linked to various organic matter degradation pathways and secondary re-oxidation reactions. In the presence of oxygen, aerobic respiration is used to break down organic matter:



where we assume organic matter (OM) to be of Redfield elemental composition (Redfield, 1958). This reaction essentially generates A_7 by the consumption of protons linked to ammonium release, and to a lesser extent, it consumes A_7 by the release of phosphate. Thamdrup and Canfield (2000) have estimated that aerobic respiration accounts for between 5–25% of the total benthic mineralization in shelf and coastal sediments. If we adopt a value of the benthic mineralization rate $R_{\min} = 10.0 \text{ mmol C m}^{-2} \text{ d}^{-1}$, which is the mean TOU value recorded for the SNS in September 2011 (Table 2; see also discussion below), we can estimate the aerobic respiration rate to range between 0.50 and 2.50 mmol C m⁻² d⁻¹ for the SNS (mean:

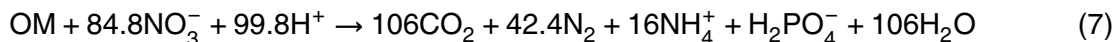
1.50 mmol C m⁻² d⁻¹). Accounting for stoichiometry (A_T/O_2 ratio = 15/106), the corresponding A_T release ranges from 0.07 to 0.35 mmol Eq m⁻² d⁻¹, with a mean of 0.21 mmol Eq m⁻² d⁻¹.

Nitrification of ammonium released during mineralization consumes A_T and can be represented by the reaction equation:



Per mole of ammonium that is released during mineralization, exactly 2 mole of A_T is consumed. If we use the TOU as a proxy for R_{\min} , the rate of ammonification (i.e. 16/106 R_{\min}) becomes 1.51 mmol N m⁻² d⁻¹ for the SNS. If all the ammonium is re-oxidized, and hence no ammonium escapes the sediment, the nitrification rate should match the ammonification rate, and so the associated A_T consumption becomes 3.02 mmol Eq m⁻² d⁻¹.

Denitrification is a second mineralization pathway via which organic matter degradation proceeds in the sediment, and can be represented as:



Per mole of organic matter denitrified, the A_T increases by 0.94 = 99.8/106 mole. To discuss the impact of denitrification on sedimentary A_T release, we need to consider the origin of the nitrate that is used for denitrification. A portion of the nitrate is internally generated in the sediment through coupled nitrification/denitrification, while another part of the nitrate is derived externally (i.e., from the overlying water column). It has been estimated that these coupled nitrification/denitrification reactions account for 80% of the total denitrification rates in coastal environments (Middelburg, 1996; Seitzinger et al., 2006), which thus implies that the total denitrification rate should scale as 1/0.8 times the nitrification rate. This way, we obtain a denitrification rate of 1.89 mmol C m⁻² d⁻¹, with an associated A_T release of 1.78 mmol Eq m⁻² d⁻¹. In the North Sea, a tight coupling of nitrification and denitrification has indeed been reported

BGD

12, 12395–12453, 2015

The impact of sedimentary alkalinity release on the water column CO₂ system

H. Brenner et al.

Title Page

Abstract

Introduction

Conclusions

References

Tables

Figures

◀

▶

◀

▶

Back

Close

Full Screen / Esc

Printer-friendly Version

Interactive Discussion



The impact of sedimentary alkalinity release on the water column CO₂ system

H. Brenner et al.

Title Page

Abstract

Introduction

Conclusions

References

Tables

Figures

◀

▶

◀

▶

Back

Close

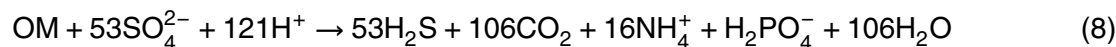
Full Screen / Esc

Printer-friendly Version

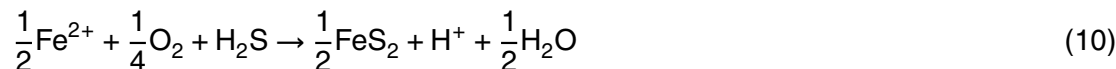
Interactive Discussion

by Lohse et al. (1993) and Pätsch and Kühn (2008), and observed benthic denitrification rates in the SNS range from 1.6 to 4.6 mmol C m⁻² d⁻¹ (Lohse et al., 1996; Hydes et al., 1999), a range that centrally embraces our estimate here. Note that the coupling of ammonification, nitrification and subsequently denitrification does not lead to *net* production of A₇. Only if nitrate is derived from the overlying water column, one obtains a net production of A₇ in the pore water (Hu and Cai, 2011a).

Once nitrate and oxygen are fully consumed, dissimilatory iron reduction and sulfate reduction are the prevailing respiration pathways (in the SNS we assume manganese oxides to be a minor electron acceptor, and so we ignore this pathway).



Both reactions are consuming protons, and hence producing A₇. Per mole organic carbon oxidized, sulfate- and iron reduction are releasing 1.14 and 8.14 moles of A₇ respectively. However, to assess the *net* A₇ generation in the sediment, we need to take the fate of the reduced species into account. The free sulphide that is generated by sulfate reduction can follow two major pathways. Some of the free sulphide (fraction ρ) will react with the reduced iron liberated by iron reduction to form pyrite. Due to its thermodynamic stability, pyrite is considered to be the primary sink for both iron and sulfur on the time scales of early diagenesis (Hu and Cai, 2011a). The overall process of pyrite formation can be represented by the reaction equation:



The remaining part of the free sulphide generated by sulfate reduction (fraction 1 – ρ) is transported upwards towards the oxic zone and re-oxidized with oxygen



The impact of sedimentary alkalinity release on the water column CO₂ system

H. Brenner et al.

Title Page

Abstract

Introduction

Conclusions

References

Tables

Figures

◀

▶

◀

▶

Back

Close

Full Screen / Esc

Printer-friendly Version

Interactive Discussion

Both pyrite formation and free sulfide reoxidation consume alkalinity. However, when combined with the alkalinity impact of sulfate reduction, pyrite formation results in a *net* generation of alkalinity, while the alkalinity consumed in free sulfide reoxidation exactly compensates the alkalinity generated during sulfate reduction. Thamdrup et al. (1994) calculated for sediments of the Aarhus Bay that the burial of reduced sulfur accounts for only 20 % of the total sulfate reduction rate, and similar values are reported in other studies (Jørgensen, 1977; Berner and Westrich, 1985; Jørgensen et al., 1990). The sediments of SNS are generally coarser and more permeable than those of Aarhus Bay, which leads to more advection and reoxygenation, which favors sulfide reoxidation as opposed to pyrite formation. Therefore, here we adopt a reduced degree of pyrite formation ($p = 0.1$; Table 1).

Adopting steady state, our simplified diagenetic model provides a set of linear relations (Table 5), which generate a particular division of the total organic matter mineralization into aerobic respiration (15 %), denitrification (24 %), iron reduction (0.4 %) and sulfate reduction (61 %). These estimates are comparable to the model analysis of Krumins et al. (2013), who estimated that sulfate reduction is the main respiratory pathway on continental shelves, accounting for 77–85 % of the organic matter mineralization, followed by aerobic respiration (16 %), denitrification (2–4 %) and iron-reduction (0.3–0.7 %). Similarly, Nedwell et al. (1993) estimated that sulfate reduction accounted for 10–53 % of the total organic matter mineralization in the SNS, while a coupled benthic–pelagic model for the North Sea suggests that up to 30 % of the organic matter is mineralized using sulfate as the electron acceptor (Luff and Moll, 2004). The TOU rate predicted by the model ($10.1 \text{ mmol O}_2 \text{ m}^{-2} \text{ d}^{-1}$) agrees well with the mean TOU observed in the SNS in September 2011 ($10.0 \text{ mmol O}_2 \text{ m}^{-2} \text{ d}^{-1}$), but the predicted respiratory coefficient (RQ = 1.26) is slightly higher than the observed one (RQ = 1.15). This higher simulated RQ could be due to an overestimate of carbonate dissolution rate, which must be reduced to $1.6 \text{ mmol C m}^{-2} \text{ d}^{-1}$ to match the observed RQ = 1.15. However, such a reduction of the carbonate dissolution rate would at the same time

lead to a substantial underprediction of the sedimentary alkalinity release, and so we stick to the carbonate dissolution rate $CD = 2.7 \text{ mmol C m}^{-2} \text{ d}^{-1}$.

Accounting for the contributions of all biogeochemical reactions, the total alkalinity generation in the sediment R_{sed} becomes (Fig. 11):

$$R_{\text{sed}} = 2r_{\text{CD}} + \frac{16-1}{106}r_{\text{AR}} + \frac{84.8+16-1}{106}r_{\text{DNF}} + \frac{848+16-1}{106}r_{\text{IR}} + \frac{106+16-1}{106}r_{\text{SR}} - 2r_{\text{NIT}} - 2r_{\text{SO}} - r_{\text{PF}}, \quad (12)$$

As we assume no alkalinity flux to deeper sediment layers, the total alkalinity generation in the sediment should match the efflux of alkalinity across the sediment–water interface. The model predicts a total alkalinity production $R_{\text{sed}} = 5.96 \text{ mmol Eq m}^{-2} \text{ d}^{-1}$, which is indeed in good agreement with the mean A_T flux of $6.50 \text{ mmol Eq m}^{-2} \text{ d}^{-1}$ as measured in our flux incubations within the SNS. Positive contributions to the A_T efflux are due to carbonate dissolution, aerobic respiration, denitrification, sulfate reduction and iron reduction, whereas A_T is consumed during nitrification, sulfur oxidation and pyrite formation. The most dominant A_T producing reaction is carbonate dissolution, followed by sulfate reduction and denitrification. The most dominant A_T consuming reactions are sulfide oxidation and nitrification. The A_T contribution of iron reduction is small and balances that of pyrite formation.

4.5 System-wide alkalinity budget

Above we have documented how the sediments of the SNS can be a source of A_T for the water column of the SNS. However, before we can estimate the resulting effect of this benthic A_T release on the $p\text{CO}_2$ dynamics of the southern North Sea, we first need to assess the A_T balance of the water column. An efflux of A_T from the sediment does necessarily result in an increase of A_T whole system, as in the water column, some biogeochemical processes are opposing the A_T generation in the sediment. Here, we identify carbonate formation (CF), primary production (PP), aerobic respiration (AR)

The impact of sedimentary alkalinity release on the water column CO_2 system

H. Brenner et al.

Title Page

Abstract

Introduction

Conclusions

References

Tables

Figures

◀

▶

◀

▶

Back

Close

Full Screen / Esc

Printer-friendly Version

Interactive Discussion



and nitrogen fixation (NF) as processes that potentially produce or consume alkalinity in the water column.

As shown above, the dissolution of carbonates in the sediment (Eq.) forms a strong source of A_T , but the production of carbonates in the water column has the opposite effect on A_T .



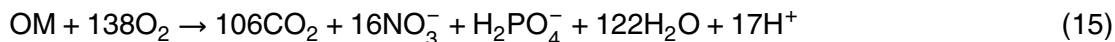
If the annual production of carbonate in the water column matches the carbonate dissolution in the sediments, there will be no net generation of A_T on a system wide scale over a whole seasonal cycle. Note however that when there is a temporal shift in production vs. dissolution of carbonates, these processes may still have an impact on the coastal A_T balance on shorter time scales. Here we assume that no net burial or export of solid carbonates occurs in the SNS on an annual scale (de Haas et al., 2002; Thomas et al., 2005; Bozec et al., 2006). Accordingly, the annual benthic carbonate dissolution must be fully compensated by carbonate production in the water column, hence carbonate production in the water column will consume $5.4 \text{ mmol Eq m}^{-2} \text{ d}^{-1}$ of A_T .

A second process which consumes alkalinity in the water column is primary production. This occurs mostly pelagic, but also benthic in some very shallow waters of the SNS. If we assume that nitrate is the main nitrogen source, primary production can be described by the reaction equation:



Joint and Pomroy (1993) estimated primary production in the southern North Sea to be $199 \text{ g C m}^{-2} \text{ yr}^{-1}$, or equally, $45.45 \text{ mmol C m}^{-2} \text{ d}^{-1}$, thus producing $7.28 \text{ mmol Eq m}^{-2} \text{ d}^{-1}$ of A_T .

Aerobic respiration in the water column can be described by the opposite reaction equation of primary production:



12423

BGD

12, 12395–12453, 2015

The impact of
sedimentary
alkalinity release on
the water column
 CO_2 system

H. Brenner et al.

Title Page

Abstract

Introduction

Conclusions

References

Tables

Figures

◀

▶

◀

▶

Back

Close

Full Screen / Esc

Printer-friendly Version

Interactive Discussion



The impact of sedimentary alkalinity release on the water column CO₂ system

H. Brenner et al.

Title Page

Abstract

Introduction

Conclusions

References

Tables

Figures

◀

▶

◀

▶

Back

Close

Full Screen / Esc

Printer-friendly Version

Interactive Discussion

To estimate the total respiration rate we need to account for two different sources of the organic matter that is being respired. The majority of the organic matter is derived from local primary production, while a smaller part originates from riverine input of terrestrial compounds. It has been estimated that about 80 % of the locally produced organic matter respire

5 in the water column, whereas the remaining 20 % sinks down to the sediments (Radach and Moll, 1993; Moll, 1998). The value of $R_{\min} = 10 \text{ mmol m}^{-2} \text{ d}^{-1}$ as derived in the previous section, compare well with this assessment, as it comes down to 22 % of the PP value of $45 \text{ mmol C m}^{-2} \text{ d}^{-1}$ as estimated above. The pelagic mineralization rate derived from local net primary production hence becomes $35 \text{ mmol C m}^{-2} \text{ d}^{-1}$.

10 Additionally, organic matter input from land also fuels respiration, either in the water column or in the benthic compartment. The total riverine input of organic matter in the SNS was estimated by Kühn et al. (2010) to be in the range of $1.0 \text{ mmol C m}^{-2} \text{ d}^{-1}$, which is hence small compared to the local net primary production. Accordingly, the total respiration rate in the water column must be $36.45 \text{ mmol C m}^{-2} \text{ d}^{-1}$, thus consuming

15 $5.85 \text{ mmol Eq m}^{-2} \text{ d}^{-1}$ of A_T .

Finally, the loss of fixed nitrogen due to denitrification in the sediment can be compensated by nitrogen fixation in the water column. However, the salinity of the North Sea is too high for diazotrophic cyanobacteria and too cold for open ocean cyanobacteria (Stal, 2009). Thus, we consider N_2 fixation in the North Sea to be negligible.

20 Similar as was done for the sediment, we can define the total alkalinity generation in the water column R_{wc} as:

$$R_{\text{wc}} = \frac{17}{106} r_{\text{PP}} - \frac{17}{106} r_{\text{AR}} - 2r_{\text{CF}} - r_{\text{NF}}, \quad (16)$$

which hence leads to a total consumption of $3.96 \text{ mmol Eq m}^{-2} \text{ d}^{-1}$ of A_T .

Based on the analysis above, we can now write an alkalinity balance for combined the sediment and water column of the SNS:

$$V_{\text{sed}} \frac{dA_T^{\text{sed}}}{dt} = -F_{\text{sed}} + R_{\text{sed}} \quad (17)$$

$$V_{\text{wc}} \frac{dA_T^{\text{wc}}}{dt} = F_{\text{river}} + F_{\text{sed}} - F_{\text{out}} + R_{\text{wc}} \quad (18)$$

5 In steady state, the net generation of alkalinity amounts to $R_{\text{net}} = R_{\text{sed}} + R_{\text{wc}} = 5.96 - 3.96 = 2.00 \text{ mmolEq m}^{-2} \text{ d}^{-1}$ or $139 \text{ GmolEq yr}^{-1}$. As shown in Table 5, 33% can be attributed to sulfur and iron cycling (i.e., anoxic mineralization taking place in the sediment) and the remaining 68% is linked to nitrogen cycling (this part is dominated by denitrification in the sediment). Furthermore, the riverine input of alkalinity was estimated by Pätsch and Kühn (2008) as $F_{\text{river}} = 1.5 \text{ mmolEq m}^{-2} \text{ d}^{-1}$, based on a river load compilation for the years 1977 to 2002. Accordingly, the A_T export flux from the SNS to the rest of the North Sea (SKNT and NNS) is $F_{\text{out}} = F_{\text{river}} + R_{\text{sed}} + R_{\text{wc}} = 1.5 + 5.96 - 3.96 = 3.50 \text{ mmol m}^{-2} \text{ d}^{-1}$ or 266 Gmol yr^{-1} .

15 As shown in Table 5, the different terms that contribute to net generation of alkalinity in the SNS have been attributed to four different types of elemental cycling (carbon, nitrogen, sulphur + iron, phosphate). This analysis reveals that no alkalinity is associated with carbon and phosphate cycling, but that 33% can be attributed to sulfur and iron cycling (i.e., anoxic mineralization taking place in the sediment) and the remaining 68% is linked to nitrogen cycling (this part is dominated by denitrification in the sediment). Sedimentary denitrification is hence the most prominent driver of net alkalinity generation in the SNS. Applying our estimated mean denitrification rate ($1.9 \text{ mmolN m}^{-2} \text{ d}^{-1}$) to the whole SNS, this implies a removal of $133 \text{ GmolN yr}^{-1}$ of bioavailable nitrogen, which closely matches the denitrification estimate of Pätsch and Kühn (2008) of $119 \text{ GmolN yr}^{-1}$ for the whole North Sea. Accounting that the sediments
20 of the SNS are the prime locations for denitrification, our estimates of denitrification
25

The impact of sedimentary alkalinity release on the water column CO₂ system

H. Brenner et al.

Title Page

Abstract

Introduction

Conclusions

References

Tables

Figures

◀

▶

◀

▶

Back

Close

Full Screen / Esc

Printer-friendly Version

Interactive Discussion



rates and the associated alkalinity generation rate in the SNS seems to be in line with previous studies.

4.6 Impact on water column $p\text{CO}_2$ dynamics of the SNS

Figure 12 shows the associated DIC and A_T budget of the water column in SNS. The direction of a CO_2 flux between the surface water and the atmosphere is determined by the $p\text{CO}_2$ gradient between water and atmosphere, which is ultimately governed by the ratio of internal DIC over internal A_T release (Frankignoulle, 1994; Egleston et al., 2010; Hu and Cai, 2011b). Assuming mean values of the SNS for the time of sampling (salinity: 34 PSU, temperature: 16.3 °C, A_T : 2270 $\mu\text{mol kg}^{-1}$) and an atmospheric CO_2 concentration of 392 ppm, one mole A_T can take up 0.85 mole atmospheric CO_2 . As shown above, the net generation of alkalinity amounts to 2.0 $\text{mmol Eq m}^{-2} \text{d}^{-1}$, and hence, 1.70 $\text{mmol C m}^{-2} \text{d}^{-1}$ of CO_2 can be taken up. However, as noted above, riverine input of organic matter and subsequent respiration of this organic matter releases 1.0 $\text{mmol C m}^{-2} \text{d}^{-1}$ of DIC. Therefore, the total atmospheric CO_2 uptake due to internal A_T generation in the SNS amounts to 1.70–1.0 = 0.70 $\text{mmol Eq m}^{-2} \text{d}^{-1}$ or 48 Gmol C yr^{-1} , which is around 6% of the total CO_2 uptake of the entire North Sea (Thomas et al., 2004; Egleston et al., 2010). This value is lower than the estimate by Thomas et al. (2009), who calculated that sedimentary A_T can potentially facilitate up to 25% of the total CO_2 uptake of the North Sea. This latter estimate was not based on direct flux measurements, but derived from an A_T budget for the North Sea, where A_T generation in Wadden Sea sediments was introduced as a closure term.

The idea that internal alkalinity generation in the SNS can drive atmospheric CO_2 uptake is further supported by previous CO_2 studies, although significant seasonality has been observed in the atmospheric CO_2 uptake. Thomas et al. (2005) reported an uptake of CO_2 for the months February to August ($-0.52 \text{ mmol C m}^{-2} \text{d}^{-1}$), while the SNS was reported to be a source for CO_2 between September and January ($+0.60 \text{ mmol C m}^{-2} \text{d}^{-1}$). Bozec et al. (2005) described the SNS as a strong

BGD

12, 12395–12453, 2015

The impact of sedimentary alkalinity release on the water column CO_2 system

H. Brenner et al.

Title Page

Abstract

Introduction

Conclusions

References

Tables

Figures

◀

▶

◀

▶

Back

Close

Full Screen / Esc

Printer-friendly Version

Interactive Discussion

**The impact of
sedimentary
alkalinity release on
the water column
CO₂ system**

H. Brenner et al.

Title Page

Abstract

Introduction

Conclusions

References

Tables

Figures

◀

▶

◀

▶

Back

Close

Full Screen / Esc

Printer-friendly Version

Interactive Discussion

- Boetius, A. and Damm, E.: Benthic oxygen uptake, hydrolytic potentials and microbial biomass at the Arctic continental slope, *Deep-Sea Res. Pt. I*, 45, 239–275, 1998. 12440
- Boon, A. R., Duineveld, G. C. A., Berghuis, E. M., and van der Weele, J. A.: Relationships between benthic activity and the annual phytopigment cycle in near-bottom water and sediments in the southern North Sea, *Estuar. Coast. Shelf S.*, 46, 1–13, 1998. 12440
- Borges, A. V. and Frankignoulle, M.: Distribution of surface carbon dioxide and air-sea exchange in the English Channel and adjacent areas, *J. Geophys. Res.-Oceans*, 108, C5, doi:10.1029/2000JC000571, 2003. 12397
- Boudreau, B. P., Middelburg, J. J., Hofmann, A. F., and Meysman, F. J.: Ongoing transients in carbonate compensation, *Global Biogeochem. Cy.*, 24, 4, doi:10.1029/2009GB003654, 2010. 12417
- Bozec, Y., Thomas, H., Elkalay, K., and de Baar, H. J. W.: The continental shelf pump for CO₂ in the North Sea – evidence from summer observation, *Mar. Chem.*, 93, 131–147, 2005. 12426
- Bozec, Y., Thomas, H., Schiettecatte, L., and Borges, A.: Assessment of the processes controlling seasonal variations of dissolved inorganic carbon in the North Sea, *Limnol. Oceanogr.*, 51, 2746–2762, 2006. 12397, 12418, 12423
- Braeckman, U., Foshtomi, M. Y., Van Gansbeke, D., Meysman, F., Soetaert, K., Vincx, M., and Vanaverbeke, J.: Variable importance of macrofaunal functional biodiversity for biogeochemical cycling in temperate coastal sediments, *Ecosystems*, 17, 720–737, 2014. 12400
- Burt, W. J., Thomas, H., Pätsch, J., Omar, A. M., Schrum, C., Daewel, U., Brenner, H., and de Baar, H. J. W.: Radium isotopes as a tracer of sediment-water column exchange in the North Sea, *Global Biogeochem. Cy.*, 28, 786–804, 2014. 12414, 12450
- Cai, W.-J. and Sayles, F. L.: Oxygen penetration depths and fluxes in marine sediments, *Mar. Chem.*, 52, 123–131, 1996. 12408, 12412
- Chen, C.-T. A.: Shelf- vs. dissolution-generated alkalinity above the chemical lysocline, *Deep-Sea Res. Pt. II*, 24, 5365–5375, 2002. 12397, 12416
- Chen, C.-T. A. and Borges, A. V.: Reconciling opposing views on carbon cycling in the coastal ocean: continental shelves as sinks and near-shore ecosystems as sources of atmospheric CO₂, *Deep-Sea Res. Pt. II*, 56, 578–590, 2009. 12396
- Chen, C. T. A. and Wang, S. L.: Carbon, alkalinity and nutrient budgets on the East China Sea continental shelf, *J. Geophys. Res.*, 104, 20675–20686, 1999. 12397, 12416
- Cramer, A.: Seasonal variation in benthic metabolic activity in a frontal system in the North Sea, *Trophic Relationships*, 1, 54–76, 1990. 12440

**The impact of
sedimentary
alkalinity release on
the water column
CO₂ system**

H. Brenner et al.

Title Page

Abstract

Introduction

Conclusions

References

Tables

Figures

◀

▶

◀

▶

Back

Close

Full Screen / Esc

Printer-friendly Version

Interactive Discussion

- Dauwe, B.: Organic matter quality in North Sea sediments, PhD thesis, Rijksuniversiteit Groningen, Groningen, The Netherlands, 1999. 12400
- de Haas, H. and van Weering, T. C.: Recent sediment accumulation, organic carbon burial and transport in the northeastern North Sea, *Mar. Geol.*, 136, 173–187, 1997. 12399
- 5 de Haas, H., van Weering, T. C. E., and de Stigter, H.: Organic carbon in shelf seas: sinks or sources, processes and products, *Cont. Shelf. Res.*, 22, 691–717, 2002. 12418, 12423
- Delvalls, T. A. and Dickson, A. G.: The pH of buffers based on 2-amino-2-hydroxymethyl-1,3-propanediol ('tris') in synthetic sea water, *Deep-Sea Res. Pt. I*, 45, 1541–1554, 1998. 12404
- 10 Denman, K. and Pena, M.: The response of two coupled one-dimensional mixed layer/planktonic ecosystem models to climate change in the NE subarctic Pacific Ocean, *Deep-Sea Res. Pt. II*, 49, 5739–5757, 2002. 12411
- Devol, A. H. and Christensen, J. P.: Benthic fluxes and nitrogen cycling in sediments of the continental margin of the eastern North Pacific, *J. Mar. Res.*, 51, 345–372, 1993. 12440
- Dickson, A. G., Sabine, C. L., and Christian, J. R.: Guide to Best Practices for Ocean CO₂ Measurements, PICES special publication, 3, North Pacific Marine Science Organization Place: Sidney, British Columbia, 2007. 12403
- 15 Egleston, E. S., Sabine, C. L., and Morel, F. M. M.: Revelle revisited: buffer factors that quantify the response of ocean chemistry to changes in DIC and alkalinity, *Global Biogeochem. Cy.*, 24, doi:10.1029/2008GB003407, 2010. 12426
- 20 Elliott, A., Clarke, T., and Li, Z.: Monthly distributions of surface and bottom temperatures in the northwest European shelf seas, *Cont. Shelf. Res.*, 11, 453–466, 1991. 12399
- Fennel, K.: The role of continental shelves in nitrogen and carbon cycling: Northwestern North Atlantic case study, *Ocean Sci.*, 6, 539–548, doi:10.5194/os-6-539-2010, 2010. 12398
- Franco, M. d. A., Vanaverbeke, J., Van Oevelen, D., Soetaert, K., Costa, M. J., Vincx, M., and Moens, T.: Respiration partitioning in contrasting subtidal sediments: seasonality and response to a spring phytoplankton deposition, *Mar. Ecol.*, 31, 276–290, 2010. 12440
- 25 Frankignoulle, M.: A complete set of buffer factors for acid/base CO₂ system in seawater, *J. Marine Syst.*, 5, 111–118, 1994. 12426
- Frankignoulle, M., Abril, G., Borges, A., Bourge, I., Canon, C., Delille, B., Libert, E., and Théate, J.-M.: Carbon dioxide emission from European estuaries, *Science*, 282, 434–436, 1998. 12417
- 30 Friedl, G., Dinkel, C., and Wehrli, B.: Benthic fluxes of nutrients in the northwestern Black Sea, *Mar. Chem.*, 62, 77–88, 1998. 12440

**The impact of
sedimentary
alkalinity release on
the water column
CO₂ system**

H. Brenner et al.

Title Page

Abstract

Introduction

Conclusions

References

Tables

Figures

◀

▶

◀

▶

Back

Close

Full Screen / Esc

Printer-friendly Version

Interactive Discussion

- Gattuso, J.-P., Frankignoulle, M., and Wollast, R.: Carbon and carbonate metabolism in coastal aquatic ecosystems, *Annu. Rev. Ecol. Syst.*, 29, 405–434, 1998. 12396
- Glud, R. N.: Oxygen dynamics of marine sediments, *Mar. Biol. Res.*, 4, 243–289, 2008. 12403, 12404, 12412
- 5 Grasshoff, K., Kremling, K., and Ehrhardt, M.: *Methods of Seawater Analysis*, John Wiley & Sons, Hoboken, New Jersey, 2009. 12402
- Grebmeier, J. M. and McRoy, C. P.: Pelagic-benthic coupling on the shelf of the northern Bering and Chukchi Seas. I. Benthic food supply and carbon cycling, *Mar. Ecol.-Prog. Ser.*, 53, 79–91, 1989. 12440
- 10 Gustafsson, B. and Stigebrandt, A.: Dynamics of the freshwater-influenced surface layers in the Skagerrak, *J. Sea Res.*, 35, 39–53, 1996. 12399
- Gustafsson, E., Wällstedt, T., Humborg, C., Mörrth, C.-M., and Gustafsson, B. G.: External total alkalinity loads versus internal generation: the influence of nonriverine alkalinity sources in the Baltic Sea, *Global Biogeochem. Cy.*, 5, 39–53, doi:10.1002/2014GB004888, 2014. 12416
- 15 Hartnett, H., Boehme, S., Thomas, C., DeMaster, D., and Smith, C.: Benthic oxygen fluxes and denitrification rates from high-resolution porewater profiles from the western Antarctic Peninsula continental shelf, *Deep-Sea Res. Pt. II*, 55, 2415–2424, 2008. 12440
- Hu, X. and Cai, W.-J.: An assessment of ocean margin anaerobic processes on oceanic alkalinity budget, *Global Biogeochem. Cy.*, 25, 3, doi:10.1029/2010GB003859, 2011a. 12398, 12416, 12420
- 20 Hu, X. and Cai, W.-J.: The impact of denitrification on the atmospheric CO₂ uptake potential of seawater, *Mar. Chem.*, 127, 192–198, 2011b. 12426
- Huettel, M. and Gust, G.: Solute release mechanisms from confined sediment cores in stirred benthic chambers and flume flows, *Mar. Ecol.-Prog. Ser.*, 82, 187–197, 1992. 12401, 12402
- 25 Huettel, M. and Rusch, A.: Transport and degradation of phytoplankton in permeable sediment, *Limnol. Oceanogr.*, 45, 534–549, 2000. 12411, 12412
- Hydes, D. J., Kelly-Gerrey, B. A., Gall, A. C. L., and Proctor, R.: The balance of supply of nutrients and demands of biological production and denitrification in a temperate latitude shelf sea – a treatment of the southern North Sea as an extended estuary, *Mar. Chem.*, 68, 117–131, 1999. 12420, 12438
- 30 Jahnke, R. A. and Jahnke, D. B.: Calcium carbonate dissolution in deep sea sediments: reconciling microelectrode, pore water and benthic flux chamber results, *Geochim. Cosmochim. Ac.*, 68, 47–59, 2004. 12418

**The impact of
sedimentary
alkalinity release on
the water column
CO₂ system**

H. Brenner et al.

Title Page

Abstract

Introduction

Conclusions

References

Tables

Figures

◀

▶

◀

▶

Back

Close

Full Screen / Esc

Printer-friendly Version

Interactive Discussion

- Lehrter, J. C., Beddick, D. L., Devereux, R., Yates, D. F., and Murrell, M. C.: Sediment-water fluxes of dissolved inorganic carbon, O₂, nutrients, and N₂ from the hypoxic region of the Louisiana continental shelf, *Biogeochemistry*, 109, 233–252, 2011. 12401
- Lenhart, H. and Pohlmann, T.: The ICES boxes approach in relation to results of a North Sea circulation model, *Tellus A*, 49, 139–160, 1997. 12399
- Liu, J., Weinbauer, M. G., Maier, C., Dai, M., and Gattuso, J.-P.: Effect of ocean acidification on microbial diversity and on microbe-driven biogeochemistry and ecosystem functioning, *Aquat. Microb. Ecol.*, 61, 291–305, 2010. 12396
- Lohse, L., Malschaert, J. F. P., Slomp, C. P., Helder, W., and van Raaphorst, W.: Nitrogen cycling in North Sea sediments: interaction of denitrification and nitrification in offshore and coastal areas, *Mar. Ecol.-Prog. Ser.*, 101, 283–283, 1993. 12420
- Lohse, L., Kloosterhuis, H., Van Raaphorst, W., Helder, W., Ecol, M., Ser, P., and February, P.: Denitrification rates as measured by the isotope pairing method and by the acetylene inhibition technique in continental shelf sediments of the North Sea, *Mar. Ecol.-Prog. Ser.*, 132, 169–179, 1996. 12420
- Lüders, K.: *Sediments of the North Sea*, Special Publications of SEPM, Wilhelmshaven, Germany, 1955. 12400
- Luff, R. and Moll, A.: Seasonal dynamics of the North Sea sediments using a three-dimensional coupled sediment–water model system, *Cont. Shelf. Res.*, 24, 1099–1127, 2004. 12421
- Meysman, F. J. R., Galaktionov, O. S., Cook, P. L. M., Janssen, F., Huettel, M., and Middelburg, J. J.: Quantifying biologically and physically induced flow and tracer dynamics in permeable sediments, *Biogeosciences*, 4, 627–646, doi:10.5194/bg-4-627-2007, 2007. 12412
- Middelburg, J.: Denitrification in marine sediments: a model study, *Global Biogeochem. Cy.*, 10, 661–673, 1996. 12419
- Moll, A.: Regional distribution of primary production in the North Sea simulated by a three-dimensional model, *J. Marine Syst.*, 16, 151–170, 1998. 12410, 12424
- Nedwell, D., Parkes, R., Upton, A., and Assinder, D.: Seasonal fluxes across the sediment–water interface, and processes within sediments, *Philos. T. R. Soc. S. A*, 343, 519–529, 1993. 12421
- Nordi, G., Debes, H., and Christensen, J. T.: *Pelagic-Benthic Coupling on the Faroe Shelf: a Pilot Study*, Tech. rep., Faroe Marine Research Institute, Faroe Island, 2013. 12440

**The impact of
sedimentary
alkalinity release on
the water column
CO₂ system**

H. Brenner et al.

[Title Page](#)

[Abstract](#)

[Introduction](#)

[Conclusions](#)

[References](#)

[Tables](#)

[Figures](#)

[◀](#)

[▶](#)

[◀](#)

[▶](#)

[Back](#)

[Close](#)

[Full Screen / Esc](#)

[Printer-friendly Version](#)

[Interactive Discussion](#)



Pätsch, J. and Kühn, W.: Nitrogen and carbon cycling in the North Sea and exchange with the North Atlantic – model study. Part I. Nitrogen budget and fluxes, *Cont. Shelf. Res.*, 28, 767–787, 2008. 12399, 12420, 12425

Osinga, R., Kop, A. J., Duineveld, G. C. A., Prins, R. A., Duyl, F. C. V., and Fleur, C.: Benthic mineralization rates at two locations in the southern North Sea, *J. Sea Res.*, 36, 181–191, 1996. 12440

Paulmier, A., Kriest, I., and Oschlies, A.: Stoichiometries of remineralisation and denitrification in global biogeochemical ocean models, *Biogeosciences*, 6, 923–935, doi:10.5194/bg-6-923-2009, 2009. 12414

Provoost, P., Braeckman, U., Van Gansbeke, D., Moodley, L., Soetaert, K., Middelburg, J. J., and Vanaverbeke, J.: Modelling benthic oxygen consumption and benthic-pelagic coupling at a shallow station in the southern North Sea, *Estuar. Coast. Shelf S.*, 120, 1–11, 2013. 12440

Radach, G. and Moll, A.: Estimation of the variability of production by simulating annual cycles of phytoplankton in the central North Sea, *Prog. Oceanogr.*, 31, 339–419, 1993. 12424

Rao, A. M., Polerecky, L., Ionescu, D., Meysman, F. J. R., and De Beer, D.: The influence of pore-water advection, benthic photosynthesis, and respiration on calcium carbonate dynamics in reef sands, *Limnol. Oceanogr.*, 28, 602–613, 2012. 12402

Rao, A. M., Malkin, S. Y., Montserrat, F., and Meysman, F. J. R.: Alkalinity production in intertidal sands intensified by lugworm bioirrigation, *Estuar. Coast. Shelf S.*, 148, 36–47, 2014. 12411

Redfield, A.: The biological control of chemical factors in the environment, *Am. Sci.*, 46, 205–221, 1958. 12413, 12418

Regnier, P., Friedlingstein, P., Ciais, P., Mackenzie, F. T., Gruber, N., Janssens, I. A., Laruelle, G. G., Lauerwald, R., Luysaert, S., Andersson, A. J., Arndt, S., Arnosti, C., Borges, A. V., Dale, A. W., Gallego-Sala, A., Godd ris, Y., Goossens, N., Hartmann, J., Heinze, C., Ilyina, T., Joos, F., LaRowe, D. E., Leifeld, J., Meysman, F. J. R., Munhoven, G., Raymond, P. A., Spahni, R., Suntharalingam, P., and Thullner, M.: Anthropogenic perturbation of the carbon fluxes from land to ocean, *Nat. Geosci.*, 6, 597–607, 2013. 12396

Reid, P. C. and Edwards, M.: Long-term changes in the pelagos, benthos and fisheries of the North Sea, *Senck. Marit.*, 31, 107–115, 2001. 12399

Rodhe, J.: The large-scale circulation in the Skagerrak; interpretation of some observations, *Tellus A*, 39, 245–253, 1987. 12399

**The impact of
sedimentary
alkalinity release on
the water column
CO₂ system**

H. Brenner et al.

Title Page

Abstract

Introduction

Conclusions

References

Tables

Figures

◀

▶

◀

▶

Back

Close

Full Screen / Esc

Printer-friendly Version

Interactive Discussion

- Rodhe, J.: On the dynamics of the large-scale circulation of the Skagerrak, *J. Sea Res.*, 35, 9–21, 1996. 12399
- Santschi, P. H., Anderson, R. F., Fleisher, M. Q., and Bowles, W.: Measurements of diffusive sublayer thicknesses in the ocean by alabaster dissolution, and their implications for the measurements of benthic fluxes, *J. Geophys. Res.-Oceans*, 96, 10641–10657, 1991. 12401
- Schiettecatte, L.-S., Thomas, H., Bozec, Y., and Borges, A. V.: High temporal coverage of carbon dioxide measurements in the Southern Bight of the North Sea, *Mar. Chem.*, 106, 161–173, 2007. 12397
- Schlüter, M. and Jerosch, K.: Digital Atlas of the North Sea, Alfred Wegener Institute for Polar and Marine Research et al., Bremerhaven, Germany, 2009. 12400
- Schrum, C., Alekseeva, I., and John, M. S.: Development of a coupled physical–biological ecosystem model ECOSMO: Part I: Model description and validation for the North Sea, *J. Marine Syst.*, 61, 79–99, 2006. 12411
- Seitzinger, S., Harrison, J., Böhlke, J., Bouwman, A., Lowrance, R., Peterson, B., Tobias, C., Van Drecht, G., Sciences, C., Brunswick, N., Survey, U. S. G., Agency, A., Watershed, S., and Hole, W.: Denitrification across landscapes and waterscapes: a synthesis, *Ecol. Appl.*, 16, 2064–2090, 2006. 12419
- Shum, K.: Wave-induced advective transport below a rippled water-sediment interface, *J. Geophys. Res.-Oceans*, 97, 789–808, 1992. 12412
- Smith Jr, K.: Oxygen demands of San Diego Trough sediments: an in situ study, *Limnol. Oceanogr.*, 19, 939–944, 1974. 12440
- Soetaert, K., Petzoldt, T., and Meysman, F.: marelac: Tools for Aquatic Sciences, R package version 2.14, available at: <http://cran.r-project.org/web/packages/marelac>, 2010. 12405
- Stal, L. J.: Is the distribution of nitrogen-fixing cyanobacteria in the oceans related to temperature?, *Environ. Microbiol.*, 11, 1632–1645, 2009. 12424
- Tengberg, A., Hall, P. O. J., Andersson, U., Lindén, B., Styrenius, O., Boland, G., de Bovee, F., Carlsson, B., Ceradini, S., Devol, A., Duineveld, G., Friemann, J.-U., Glud, R. N., Khripounoff, A., Leather, J., Linke, P., Lund-Hansen, L., Rowe, G., Santschi, P., de Wilde, P., and Witte, U.: Intercalibration of benthic flux chambers, *Mar. Chem.*, 94, 147–173, 2005. 12401
- Thamdrup, B. and Canfield, D. E.: Benthic respiration in aquatic sediments, in: *Methods in Ecosystem Science*, Springer, New York, 86–103, 2000. 12410, 12418

**The impact of
sedimentary
alkalinity release on
the water column
CO₂ system**

H. Brenner et al.

[Title Page](#)[Abstract](#)[Introduction](#)[Conclusions](#)[References](#)[Tables](#)[Figures](#)[⏪](#)[⏩](#)[◀](#)[▶](#)[Back](#)[Close](#)[Full Screen / Esc](#)[Printer-friendly Version](#)[Interactive Discussion](#)

Thamdrup, B., Fossing, H., and Jørgensen, B. B.: Manganese, iron and sulfur cycling in a coastal marine sediment, Aarhus Bay, Denmark, *Geochim. Cosmochim. Ac.*, 58, 5115–5129, 1994. 12421

Therkildsen, M. S. and Lomstein, B. A.: Seasonal variation in net benthic C-mineralization in a shallow estuary, *FEMS Microbiol. Ecol.*, 12, 131–142, 1993. 12413

Thomas, H., Bozec, Y., Elkalay, K., and de Baar, H. J. W.: Enhanced open ocean storage of CO₂ from shelf sea pumping, *Science*, 304, 1005–1008, 2004. 12426

Thomas, H., Bozec, Y., de Baar, H. J. W., Elkalay, K., Frankignoulle, M., Schiettecatte, L.-S., Kattner, G., and Borges, A. V.: The carbon budget of the North Sea, *Biogeosciences*, 2, 87–96, doi:10.5194/bg-2-87-2005, 2005. 12418, 12423, 12426

Thomas, H., Schiettecatte, L.-S., Suykens, K., Koné, Y. J. M., Shadwick, E. H., Prowe, A. E. F., Bozec, Y., de Baar, H. J. W., and Borges, A. V.: Enhanced ocean carbon storage from anaerobic alkalinity generation in coastal sediments, *Biogeosciences*, 6, 267–274, doi:10.5194/bg-6-267-2009, 2009. 12397, 12415, 12426, 12438

Trimmer, M., Nedwell, D., Sivyer, D., and Malcolm, S.: Seasonal benthic organic matter mineralisation measured by oxygen uptake and denitrification along a transect of the inner and outer River Thames estuary, UK, *Mar. Ecol.-Prog. Ser.*, 197, 103–119, 2000. 12440

Trimmer, M., Petersen, J., Sivyer, D., Mills, C., Young, E., and Parker, E.: Impact of long-term benthic trawl disturbance on sediment sorting and biogeochemistry in the southern North Sea, *Mar. Ecol.-Prog. Ser.*, 298, 79–94, 2005. 12440

Upton, A.: Seasonal benthic microbial activity in the southern North Sea; oxygen uptake and sulphate reduction, *Mar. Ecol. Progr. Ser.*, 101, 273–281, 1993. 12440

Van der Molen, J.: The influence of tides, wind and waves on the net sand transport in the North Sea, *Cont. Shelf. Res.*, 22, 2739–2762, 2002. 12400

van Duyl, F. C., Bak, R. P. M., Kop, A. J., Nieuwland, G., Berghuis, E. M., and Kok, A.: Mesocosm experiments: mimicking seasonal developments of microbial variables in North Sea sediments, *Hydrobiologia*, 235, 267–281, 1992. 12440

Van Raaphorst, W., Kloosterhuis, H. H. T., Cramer, A., and Bakker, K. J. M.: Nutrient early diagenesis in the sandy sediments of the Dogger Bank area, North Sea: pore water results, *Neth. J. Sea Res.*, 26, 25–52, 1990. 12440

Weston, K., Fernand, L., Nicholls, J., Marca-Bell, A., Mills, D., Sivyer, D., and Trimmer, M.: Sedimentary and water column processes in the Oyster Grounds: a potentially hypoxic region of the North Sea, *Marine Environ. Res.*, 65, 235–249, 2008. 12440

Wilde, P., Berghuis, E., and Kok, A.: Structure and energy demand of the benthic community of the Oyster Ground, central North Sea, Neth. J. Sea Res., 18, 143–159, 1984. 12440
Witte, U. and Pfannkuche, O.: High rates of benthic carbon remineralisation in the abyssal Arabian Sea, Deep-Sea Res. Pt. II, 47, 2785–2804, 2000. 12440

BGD

12, 12395–12453, 2015

The impact of sedimentary alkalinity release on the water column CO₂ system

H. Brenner et al.

Title Page

Abstract

Introduction

Conclusions

References

Tables

Figures

◀

▶

◀

▶

Back

Close

Full Screen / Esc

Printer-friendly Version

Interactive Discussion



The impact of sedimentary alkalinity release on the water column CO₂ system

H. Brenner et al.

[Title Page](#)[Abstract](#)[Introduction](#)[Conclusions](#)[References](#)[Tables](#)[Figures](#)[⏪](#)[⏩](#)[◀](#)[▶](#)[Back](#)[Close](#)[Full Screen / Esc](#)[Printer-friendly Version](#)[Interactive Discussion](#)**Table 2.** Fluxes at the sediment–water interface for O₂ (TOU), A_T and DIC.

		September 2011		June 2012		Literature	
		Mean	Range	Mean	Range	Mean	Range
TOU	SNS	10.0 ± 2.4	3.1–28.7	13.5 ± 4.5	6.5–25.1	14.9 ^a	5.2–28.4 ^a
	NNS	3.4 ± 0.4	0.7–6.2	–	–	–	–
	SKNT	3.9 ± 0.4	2.9–5.7	–	–	–	–
A _T flux	SNS	6.5 ± 5.2	0–21.4	5.7 ± 3.7	0.5–18.7	9.6 ^b	–
	NNS	1.8 ± 2.4	0–3	–	–	–	–
	SKNT	4.3 ± 3.3	1.4–9.9	–	–	–	–
DIC flux	SNS	11.5 ± 5.4	1.5–29.1	12.3 ± 2.6	–	–	–
	NNS	0.9 ± 2.1	0–6.2	–	–	–	–
	SKNT	6.14 ± 2.6	4.2–7.4	–	–	–	–

^a Hydes et al. (1999).^b Thomas et al. (2009).Units mmol C m⁻² d⁻¹ (DIC flux); mmol Eq m⁻² d⁻¹ (A_T flux); mmol O₂ m⁻² d⁻¹ (TOU rate).

The impact of sedimentary alkalinity release on the water column CO₂ system

H. Brenner et al.

Title Page

Abstract

Introduction

Conclusions

References

Tables

Figures

◀

▶

◀

▶

Back

Close

Full Screen / Esc

Printer-friendly Version

Interactive Discussion

Table 3. Comparison between TOU rates as measured by FireSting optodes and diffusive oxygen uptake rates (DOU) obtained from O₂ microprofiles.

Station	TOU	DOU	OPD
11	10.02	0.20	NA
20	22.40	2.07	5.30
30	11.33	6.95	1.10
38	3.73	1.06	13.30
45	7.32	1.67	NA
52	5.49	0.83	17.00
56	3.76	1.47	NA
59	4.94	4.33	3.20
62	4.80	2.49	NA
65	3.01	1.88	15.10
71	3.67	1.76	7.10
80	4.62	1.25	8.80
88	2.25	1.87	14.80

Unit: mmol O₂ m⁻² d⁻¹; oxygen penetration depth (OPD) for cores used for microprofiling in mm.

NA indicates that oxygen does not deplete over the measured depth.

Table 4. TOU rates ($\text{mmolO}_2 \text{m}^{-2} \text{d}^{-1}$) measured in the North Sea and other coastal systems taken from literature compared to this study.

Literature	Location	Month and year	TOU
North Sea			
Wilde et al. (1984)	OG	5, 8, 9 (1980, 1981)	3.6–14.4
Cramer (1990)	FF	5, 6 (1986), 8, 9 (1987)	23.3–51.8
Raaphorst et al. (1990)	DB	7, 8 (1988)	4–20
	BF	1, 4, 5, 8, 11 (1989)	2–22
van Duyl et al. (1992)	FF	1, 4, 5, 8, 11 (1989)	15–40
Upton (1993)	U1	9, 10 (1988), 2, 4, 6, 8, 9 (1989)	5–16
	FF	9, 10 (1988), 2, 4, 6, 8, 9 (1989)	5–28
	U3	9, 10 (1988), 2, 4, 6, 8, 9 (1989)	7–25
	U4	9, 10 (1988), 2, 4, 6, 8, 9 (1989)	10–11
	U5	9, 10 (1988), 2, 4, 6, 8, 9 (1989)	6–10
	U6	9, 10 (1988), 2, 4, 6, 8, 9 (1989)	7–18
Lohse et al. (1996)	OG	7 (1994)	5.6–6.1
Osinga et al. (1996)	BF	2 (1993), 7, 10 (1994)	< 24
	OG	2 (1993), 7, 10 (1994)	< 63
Boon et al. (1998)	BF	2, 3, 4, 6, 8, 11 (1993)	< 19.2
	FF	2, 3, 4, 6, 8, 11 (1993)	< 48
Trimmer et al. (2000)	Thms	7, 10 (1996), 4, 7 (1997)	11.4–5.8
Trimmer et al. (2005)	USP	10 (2001), 7 (2002)	16.1–57.1
	Thms	10 (2001), 7 (2002)	14–43.9
Weston et al. (2008)	OG	9 (2003)	12.6–30.6
Franco et al. (2010)	F115bis	2, 4, 10 (2003)	5.5–18.8
	F330	2, 4, 10 (2003)	1.2–8.7
Provoost et al. (2013)	F115	9, 10, 11, 12 (2002), 1, 2, 3, 4, 5, 7, 8, 9, 10 (2003)	4.5–32.9
Braeckman et al. (2014)	BM	2, 3, 4, 5, 6, 7, 8, 9 (2011)	0–41.92
	BFS	2, 3, 4, 5, 6, 7, 8, 9 (2011)	< 56.31
	BFS	10 (2011)	43.88
	BS	2, 3, 4, 5, 6, 7, 8, 9 (2011)	< 22.94
	BS	10 (2011)	6.63
Other coastal systems			
Lansard et al. (2008)	MS	06 (2001 and 2002)	3.9–25.6
Nordi et al. (2013)	FS	04 05 06 07 08 (2011) 02 06 07 (2012)	3.3–6.8
Archer et al. (1992)	WS	06 (1988)	1.0–18.3
Grebmeier and McRoy (1989)	BC	07 08 09 (1984–1986)	0.3–16.9
Smith Jr (1974)	SD	10 (1973)	0.4–3.9
Boetius and Damm (1998)	AC	08 09 (1993)	0.2–2.3
Witte and Pfannkuche (2000)	AS	10 (1995)	0.9–6.3
Devol and Christensen (1993)	WS	06 07 (1988) 06 (1991)	2.9–18.5
Berelson et al. (2003)	MB	06 (1991)–10 (1995)	5.1–13.5
Friedl et al. (1998)	BS	Summer (1995)	0.0–33.0
Hartnett et al. (2008)	AP	03 06 10 (2000) 02 (2001)	1.5–2.1
Larsen et al. (2013)	CS	07 (2008)	5.8–9.0
This study	SNS	9 (2011)	3.12–28.65
	SNS	4 (2012)	6.50–25.11
	NNS	9 (2011)	0.74–6.20

OG: Oyster Ground, FF: Frisian Front, DB: Dogger Bank, BF: Broad Fourteens, U1–U3: (near) English Channel, U4–U6: Central North Sea, F115bis, F330, BM, BFS, BS: Belgian Coast, Thms: Thames, USP: Outer Silver Pit, MS: Mediterranean Sea, FS: Faro Shelf, WS: Washington Shelf, BC: northern Bering and Chukchi Seas, SD: San Diego Trough, AC: Arctic Continental Slope, AS: Arabian Sea, MB: Monterey Bay, BS: Black Sea, AP: western Antarctic Peninsula, CS: Celtic Sea, SNS: southern North Sea, NNS: northern North Sea.

The impact of sedimentary alkalinity release on the water column CO₂ system

H. Brenner et al.

Title Page

Abstract

Introduction

Conclusions

References

Tables

Figures

◀

▶

◀

▶

Back

Close

Full Screen / Esc

Printer-friendly Version

Interactive Discussion

The impact of sedimentary alkalinity release on the water column CO₂ system

H. Brenner et al.

[Title Page](#)
[Abstract](#)
[Introduction](#)
[Conclusions](#)
[References](#)
[Tables](#)
[Figures](#)
[Back](#)
[Close](#)
[Full Screen / Esc](#)
[Printer-friendly Version](#)
[Interactive Discussion](#)


Table 5. Input parameters and rate expressions for all diagenetic and pelagic processes included in our model. Additionally, the impact of the different elemental cycles are expressed in percentages.

Input parameter	Expression	Value	Units	A _r release
Mineralization rate	Rmin	10.0	mmolCm ⁻² d ⁻¹	–
Carbonate dissolution rate	CD	2.70	mmolCm ⁻² d ⁻¹	–
Aerobic respiration fraction	a	0.15	–	–
Fraction of DNF supported by NI	b	0.8	–	–
Pyrite formation fraction	p	0.2	–	–
Pelagic processes				
Primary production	PP	45.40	mmolCm ⁻² d ⁻¹	+7.28
Aerobic respiration	AR	36.45	mmolCm ⁻² d ⁻¹	–5.85
Carbonate formation	CF	2.70	mmolCm ⁻² d ⁻¹	–5.40
Nitrogen fixation	NF	0	mmolCm ⁻² d ⁻¹	0
Alkalinity generation	See text		mmolEqm ⁻² d ⁻¹	–3.96
Diagenetic processes				
Carbonate dissolution	CD	2.70	mmolCm ⁻² d ⁻¹	+5.40
Aerobic respiration	AR = a · Rmin	1.50	mmolCm ⁻² d ⁻¹	+0.21
Nitrification	NIT = $\frac{16}{106} \cdot Rmin$	1.51	mmolCm ⁻² d ⁻¹	–3.02
Denitrification	DNF = $\frac{1}{0.8} \cdot \frac{1}{b} \cdot NIT$	1.89	mmolCm ⁻² d ⁻¹	+1.78
Sulfate reduction	SR = $\frac{Rmin - AR - DNF}{1 + \frac{p}{16}}$	6.57	mmolCm ⁻² d ⁻¹	+7.50
Pyrite formation	PF = 0.5 · p · SR	0.33	mmolCm ⁻² d ⁻¹	–0.33
Sulfide oxidation	SO = 0.5(1 – p) · SR	2.96	mmolCm ⁻² d ⁻¹	–5.91
Iron reduction	IR = $\frac{1}{16} \cdot p \cdot SR$	0.04	mmolCm ⁻² d ⁻¹	+0.33
Alkalinity generation	see text		mmolEqm ⁻² d ⁻¹	+5.96
Total oxygen uptake	TOU = AR + 2 · NIT + 2 · SO + 0.25PF	10.1	mmolO ₂ m ⁻² d ⁻¹	
Respiratory quotient	RQ = $\frac{Rmin + CD}{TOU}$	1.26		
Linked to				
Carbon cycle	2 · CD – 2 · CF	0	%	–
Nitrogen cycle	84.8/106 · DNF + 16/106 · (AR + DNF + IR + SR) – 2 · NIT + (16/106) · (PP – WAR)	68	%	–
Sulphur and iron cycle	8 · IR + SR – 2 · SO – PF	33	%	–
Phosphor cycle	–1/106 · (AR + DNF + IR + SR) + (1/106) · (PP – WAR)	0	%	–

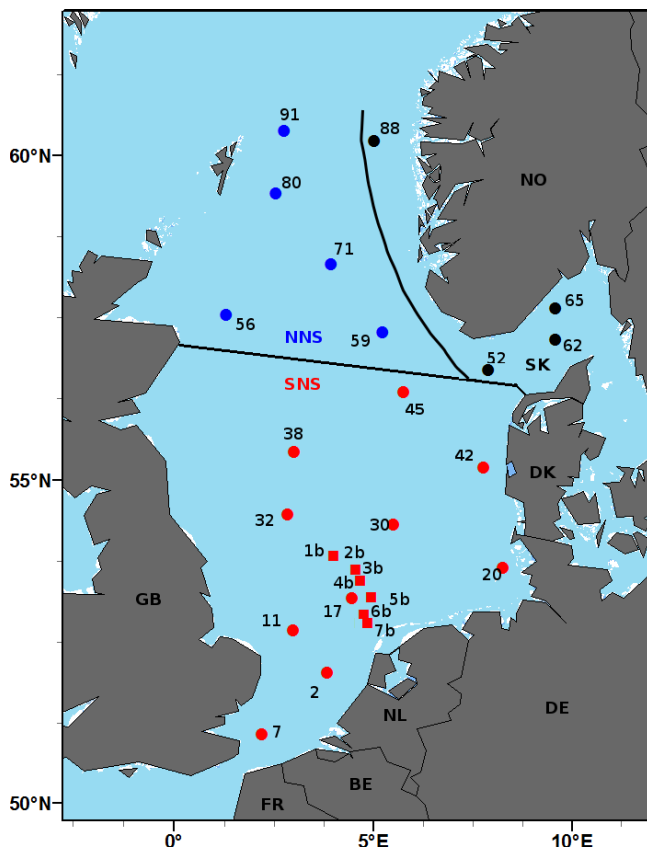


Figure 1. Map of sampled stations. Red symbols: southern North Sea, black symbols: Skagerrak, blue symbols: northern North Sea, circles: sampled in September 2011, squares: sampled in June 2012. Border of the Skagerrak as defined by the International Hydrographic Organization, border between SNS and NNS roughly represents the 100 m depth isoline.

The impact of sedimentary alkalinity release on the water column CO₂ system

H. Brenner et al.

[Title Page](#)

[Abstract](#)

[Introduction](#)

[Conclusions](#)

[References](#)

[Tables](#)

[Figures](#)

[⏪](#)

[⏩](#)

[◀](#)

[▶](#)

[Back](#)

[Close](#)

[Full Screen / Esc](#)

[Printer-friendly Version](#)

[Interactive Discussion](#)



The impact of sedimentary alkalinity release on the water column CO₂ system

H. Brenner et al.

[Title Page](#)

[Abstract](#)

[Introduction](#)

[Conclusions](#)

[References](#)

[Tables](#)

[Figures](#)

[⏪](#)

[⏩](#)

[◀](#)

[▶](#)

[Back](#)

[Close](#)

[Full Screen / Esc](#)

[Printer-friendly Version](#)

[Interactive Discussion](#)

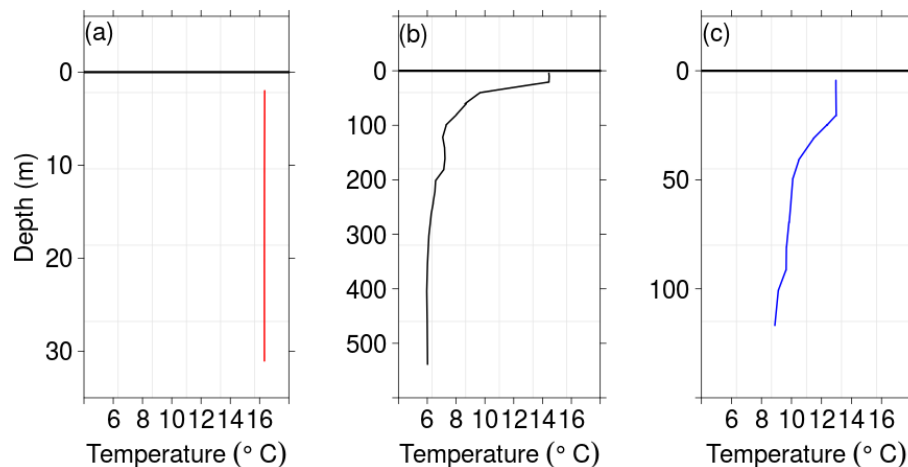


Figure 2. Temperature profiles as recorded by a CTD cast for: **(a)** Station 11 (SNS); **(b)** Station 45 (SNS); **(c)** Station 65 (SKNT); Station 80 (NNS).

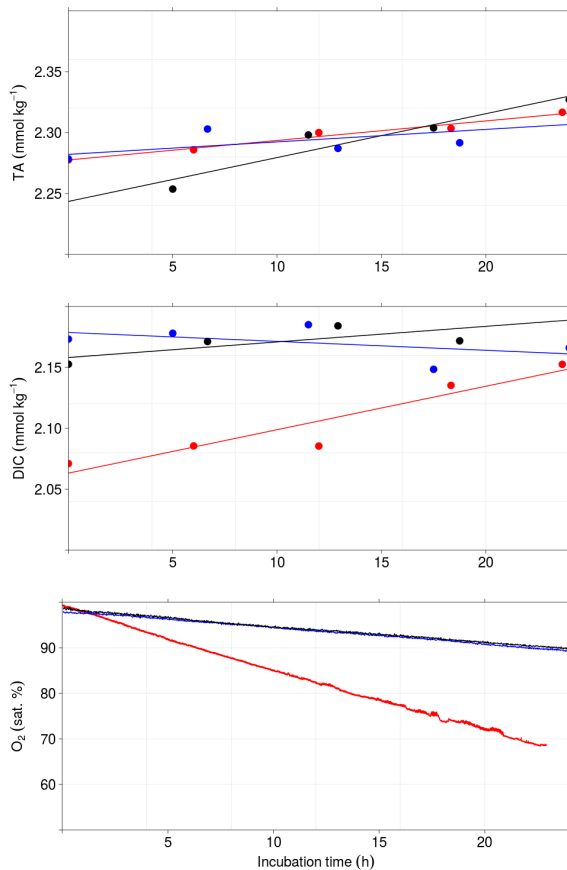


Figure 3. Representative concentrations of A_T , DIC and O_2 saturation over time for all three regions of the North Sea. Red: Station 11 (SNS); blue: Station 71 (NNS); black: Station 65 (SKNT).

The impact of sedimentary alkalinity release on the water column CO₂ system

H. Brenner et al.

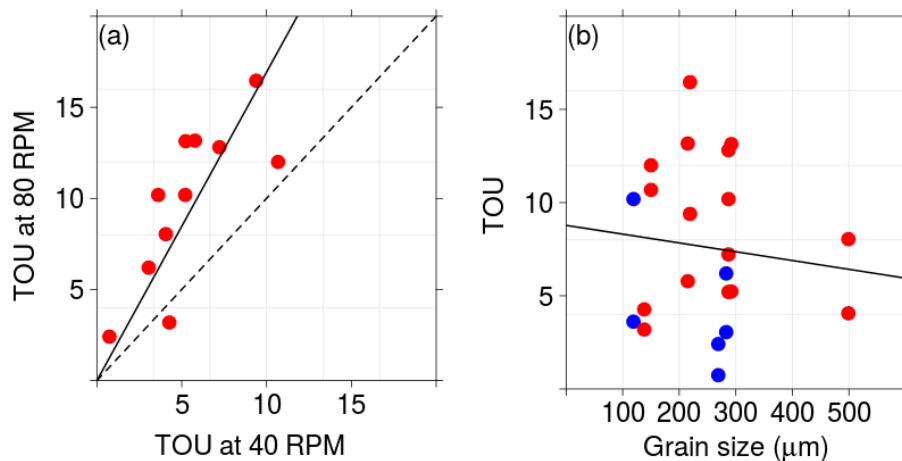


Figure 4. (a) Total oxygen uptake rates measured in benthic incubation chambers at two different stirring rates (RPM = rounds min⁻¹); (b) TOU rates in correlation to the median grain size. Dashed line: 1 : 1 line; solid line: linear regression; red symbols: SNS; blue symbols: NNS. All rates in mmol O₂ m⁻² d⁻¹.

[Title Page](#)
[Abstract](#)
[Introduction](#)
[Conclusions](#)
[References](#)
[Tables](#)
[Figures](#)
[⏪](#)
[⏩](#)
[◀](#)
[▶](#)
[Back](#)
[Close](#)
[Full Screen / Esc](#)
[Printer-friendly Version](#)
[Interactive Discussion](#)

The impact of sedimentary alkalinity release on the water column CO₂ system

H. Brenner et al.

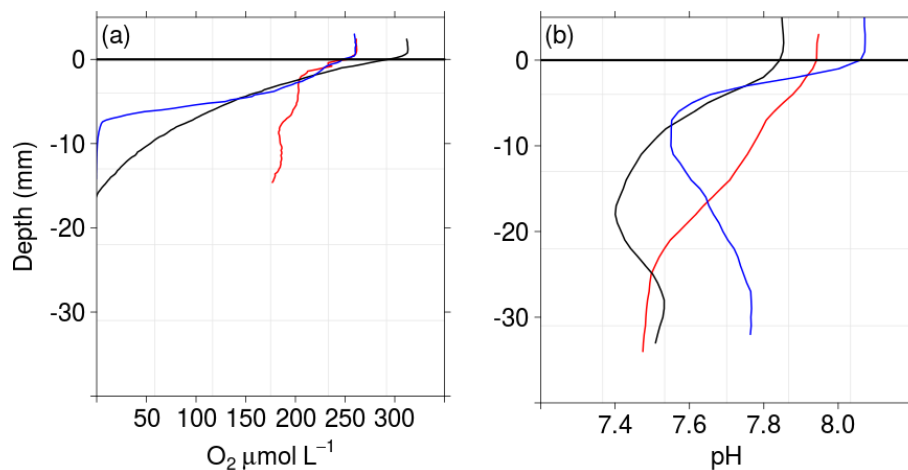


Figure 5. Examples of microsensor depth profiles from different regions of the North Sea. **(a)** O₂; **(b)** pH; red: Station 11 (SNS); blue: Station 65 (SKNT); black: Station 80 (NNS); solid line: sediment–water interface.

Title Page

Abstract

Introduction

Conclusions

References

Tables

Figures

◀

▶

◀

▶

Back

Close

Full Screen / Esc

Printer-friendly Version

Interactive Discussion

The impact of sedimentary alkalinity release on the water column CO_2 system

H. Brenner et al.

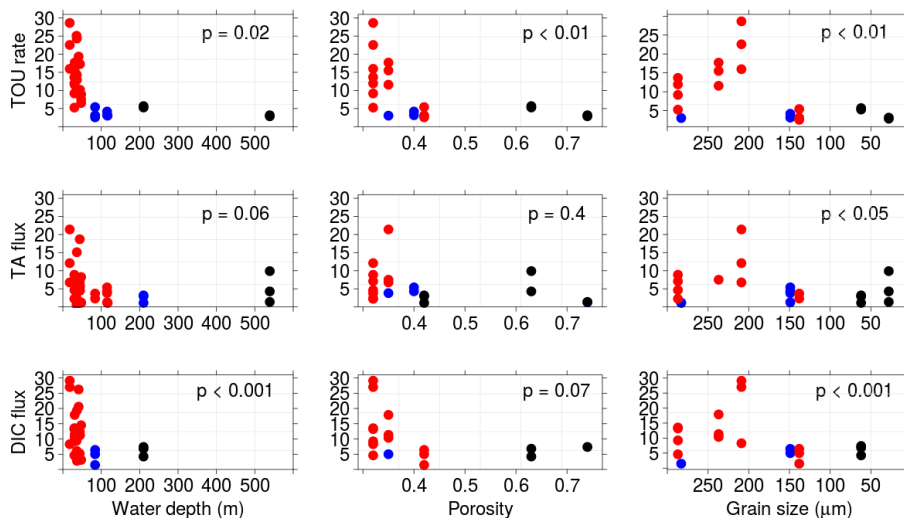


Figure 6. Correlation plots between DIC-, A_7 -fluxes, TOU rates and water depth, porosity and grain size. Red: SNS, black: SKNT, blue: NNS; Spearman's p value given in each plot. Units $\text{mmol C m}^{-2} \text{d}^{-1}$ (DIC); $\text{mmol Eq m}^{-2} \text{d}^{-1}$ (A_7); $\text{mmol O}_2 \text{m}^{-2} \text{d}^{-1}$ (TOU).

The impact of sedimentary alkalinity release on the water column CO₂ system

H. Brenner et al.

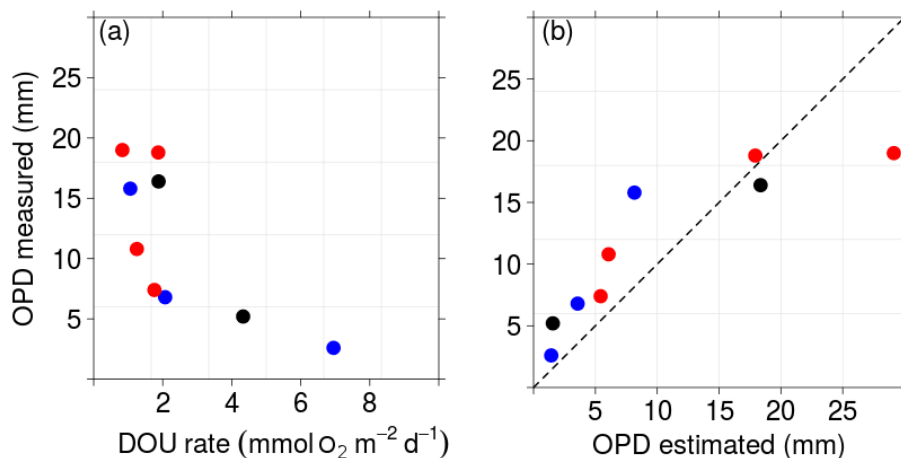


Figure 7. (a) Oxygen Penetration Depth (OPD) plotted vs. Diffusive Oxygen Uptake (DOU) rate. Filled circles: measured values; empty circles: theoretical values (b) measured OPD vs. theoretical OPD. Dashed line: 1 : 1 line; red symbols: SNS; blue symbols: NNS; black: SKNT. For calculation and details see text.

[Title Page](#)
[Abstract](#)
[Introduction](#)
[Conclusions](#)
[References](#)
[Tables](#)
[Figures](#)
[◀](#)
[▶](#)
[◀](#)
[▶](#)
[Back](#)
[Close](#)
[Full Screen / Esc](#)
[Printer-friendly Version](#)
[Interactive Discussion](#)

The impact of sedimentary alkalinity release on the water column CO_2 system

H. Brenner et al.

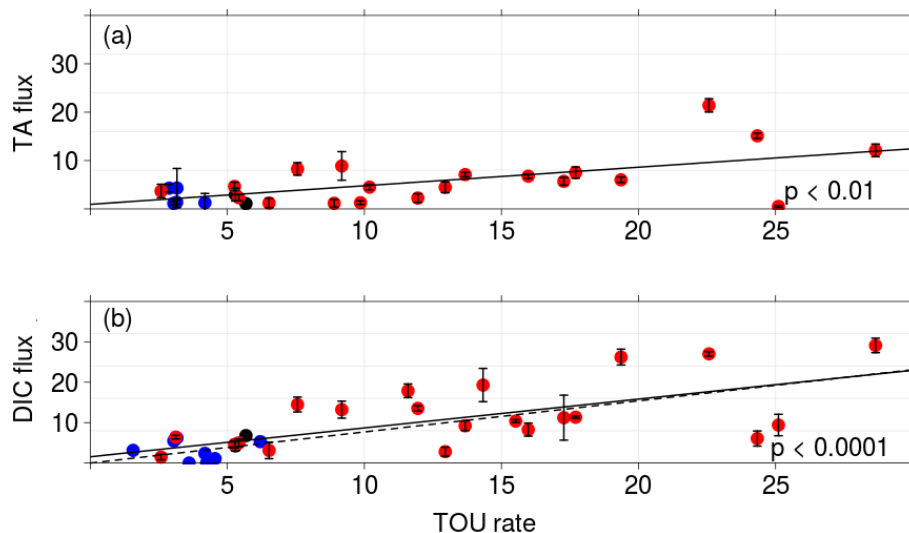


Figure 8. (a) Correlation between A_T fluxes and TOU rates. (b) Correlation between DIC fluxes and TOU rates. Dashed line: line of $RQ = 0.77$; solid line: linear regression; Spearman's ρ value given in each plot. TA and DIC fluxes in $\text{mmol C m}^{-2} \text{d}^{-1}$. TOU rates in $\text{mmol O}_2 \text{m}^{-2} \text{d}^{-1}$.

[Title Page](#)[Abstract](#)[Introduction](#)[Conclusions](#)[References](#)[Tables](#)[Figures](#)[◀](#)[▶](#)[◀](#)[▶](#)[Back](#)[Close](#)[Full Screen / Esc](#)[Printer-friendly Version](#)[Interactive Discussion](#)

The impact of
sedimentary
alkalinity release on
the water column
CO₂ system

H. Brenner et al.

Title Page

Abstract

Introduction

Conclusions

References

Tables

Figures

◀

▶

◀

▶

Back

Close

Full Screen / Esc

Printer-friendly Version

Interactive Discussion

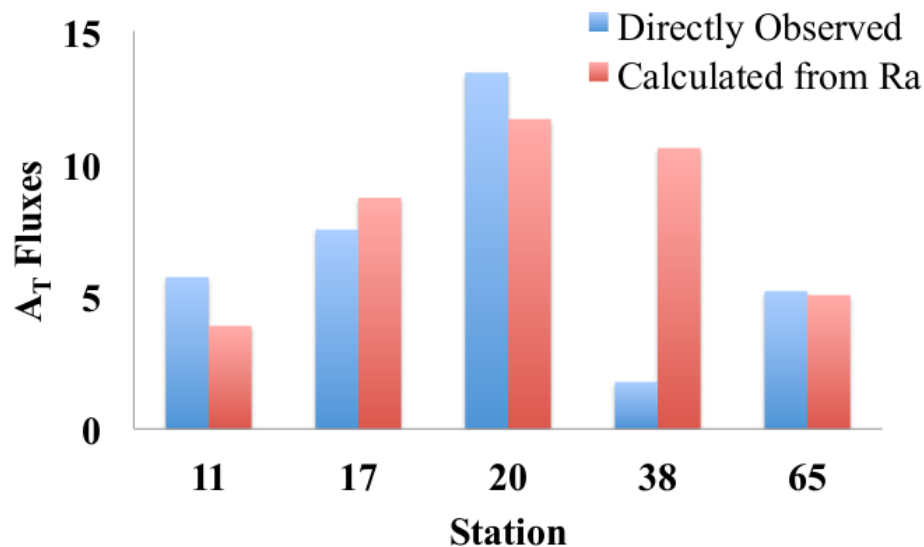


Figure 9. Directly measured A_T fluxes for the SNS compared to A_T flux estimations based on R_a measurements. Figure taken from Burt et al. (2014). Fluxes in $\text{mmol C m}^{-2} \text{d}^{-1}$.

The impact of sedimentary alkalinity release on the water column CO_2 system

H. Brenner et al.

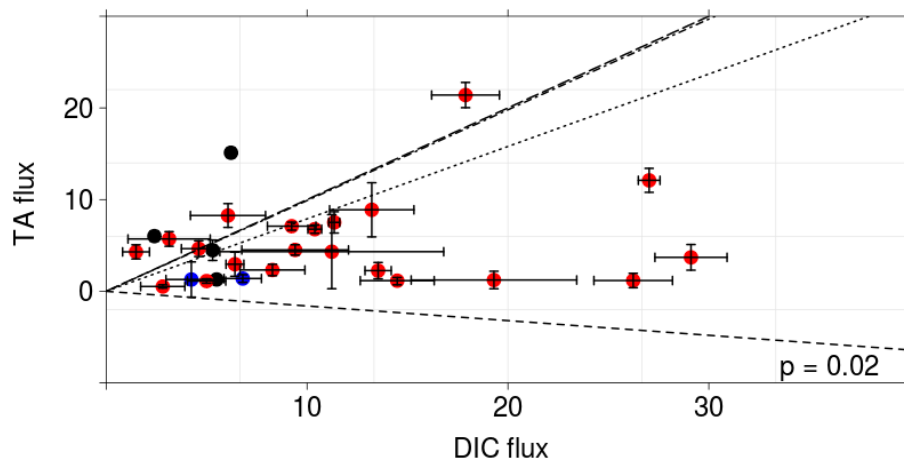


Figure 10. Correlation between A_T and DIC fluxes for sites of the SNS from both campaigns. Different lines are representing different reaction stoichiometry. For more explanation and reaction equations see text. Short dashed line: aerobic respiration; dotted line: denitrification; dotted/dashed line: sulfate reduction coupled to pyrite formation and burial; long dashed line: carbonate dissolution; ρ : Spearman's rank correlation coefficient. All fluxes in $\text{mmol Cm}^{-2} \text{d}^{-1}$.

Title Page

Abstract

Introduction

Conclusions

References

Tables

Figures

◀

▶

◀

▶

Back

Close

Full Screen / Esc

Printer-friendly Version

Interactive Discussion

The impact of sedimentary alkalinity release on the water column CO₂ system

H. Brenner et al.

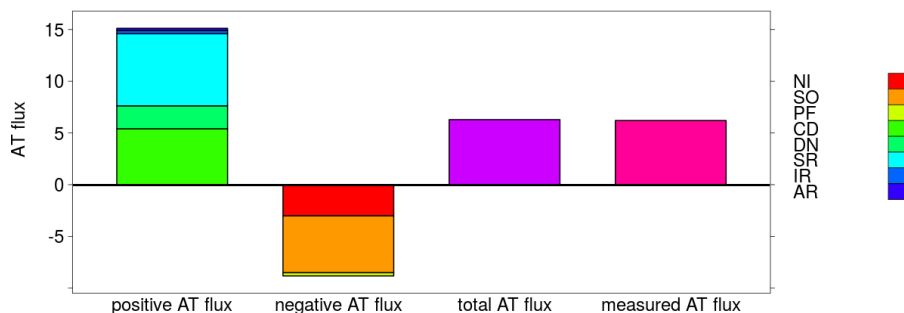


Figure 11. Contribution of different processes to the AT budget in the SNS. For more details on different reaction rates see text. NI: nitrification; SO: sulfide oxidation; PF: pyrite formation; CD: carbonate dissolution; DN: denitrification; SR: sulfate reduction; IR: dissimilatory iron reduction; AR: aerobic respiration. Fluxes in $\text{mmol C m}^{-2} \text{d}^{-1}$.

Title Page

Abstract

Introduction

Conclusions

References

Tables

Figures

◀

▶

◀

▶

Back

Close

Full Screen / Esc

Printer-friendly Version

Interactive Discussion

The impact of sedimentary alkalinity release on the water column CO_2 system

H. Brenner et al.

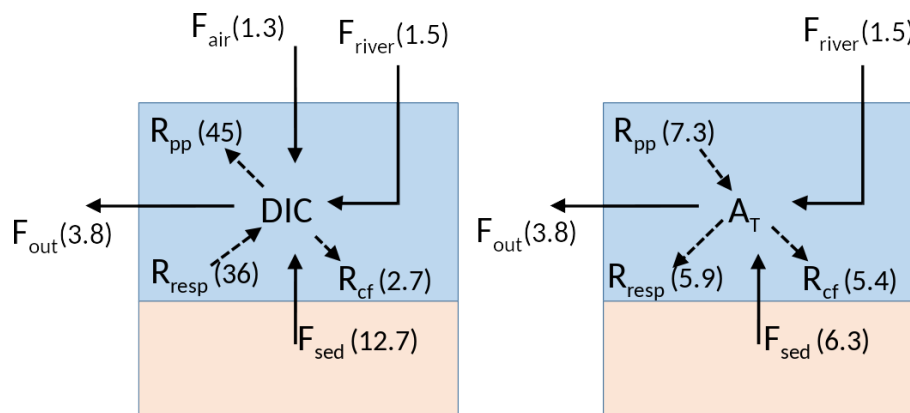


Figure 12. DIC and A_T budgets of the water column in the SNS. Bold arrows: fluxes; dashed arrows: reaction rates. F_{sed} : net flux from the sediments; F_{river} : riverine input; F_{out} : flux into the NNS/SKNT; F_{air} : atmospheric DIC uptake; R_{pp} : primary production rate; R_{resp} : aerobic respiration rate; R_{cf} : carbonate production rate. Unit: $\text{mmol C m}^{-2} \text{d}^{-1}$.